A process based model of cohesive sediment resuspension under bioturbators' influence

Cozzoli, Francesco; Gjoni, Vojsava; Del Pasqua, Michela; Hu, Zhan; Ysebaert, Tom; Herman, Peter M.J.; Bouma, T.J.

DOI
10.1016/j.scitotenv.2019.03.085

Publication date
2019

Document Version
Accepted author manuscript

Published in
Science of the Total Environment

Citation (APA)
Cozzoli, F., Gjoni, V., Del Pasqua, M., Hu, Z., Ysebaert, T., Herman, P. M. J., & Bouma, T. J. (2019). A process based model of cohesive sediment resuspension under bioturbators' influence. *Science of the Total Environment*, *670*, 18-30. https://doi.org/10.1016/j.scitotenv.2019.03.085

A process based model of cohesive sediment resuspension under bioturbators' influence

Cozzoli, Francesco[a, †]*; Gjoni, Vojsava*[a]*; Del Pasqua, Michela*[a]*; Zhan, Hu*[b, §]*; Ysebaert, Tom*[c,d]*; Herman Peter M.J*[e,f]*.; Bouma Tjeerd J*[d]

[a] Dipartimento di Scienze e Tecnologie Biologiche ed Ambientali, University of the Salento – 73100 Lecce, Italy

[b] School of Marine Science, Sun Yat-sen University, 510275 Guangzhou, China

[c] Wageningen Marine Research, Wageningen University and Research, P.B. 77, 4400 AB Yerseke, The Netherlands

[d] Department of Estuarine and Delta Systems. Royal Netherlands Institute of Sea Research (NIOZ) and Utrecht University. 4401 NT Yerseke, The Netherlands

[e]Department of Hydraulic Engineering, Delft University of Technology, 2628 CN, P.O. Box 5048 2600 GA, Delft, The Netherlands

[f] Deltares, P.O. Box 177 2600 MH, Delft, The Netherlands

[†]**Corresponding author**: Dipartimento di Scienze e Tecnologie Biologiche ed Ambientali. Centro Ecotekne Pal. B S.P. 6 Lecce – Monteroni, 73100 Lecce, Italy; francesco.cozzoli@unisalento.it

[§]**Corresponding author:** School of Marine Science, Sun Yat-sen University, 510275 Guangzhou, China; huzh9@mail.sysu.edu.cn.

Keywords: bioturbation; sediment resuspension; annular flumes; metabolism; process-based model

Abstract

Macrozoobenthos may affect sediment stability and erodibility *via* their bioturbating activities, thereby impacting both the short- and long-term development of coastal morphology. Process-based models accounting for the effect of bioturbation are needed for the modelling of erosion dynamics. With this work, we explore whether the fundamental allometric principles of metabolic activity scaling with individual and population size may provide a framework to derive general patterns of bioturbation effect on cohesive sediment resuspension. Experimental flumes were used to test this scaling approach across different species of marine, soft-sediment bioturbators. The collected dataset encompasses a range of bioturbators functional diversity, individual densities, body sizes and overall population metabolic rates. Measurements were collected on a range of hydrodynamic stress from 0.02 to 0.25 Pa.

Overall, we observed that bioturbators are able to slightly reduce the sediment resuspension at low hydrodynamic stress, whereas they noticeably enhance it at higher levels of stress. Along the whole hydrodynamic stress gradient, the quantitative effect of bioturbators on sediment resuspension can be efficiently described by the overall metabolic rate of the bioturbating benthic communities, with significant variations across the bioturbators' taxonomic and functional diversity. One of the tested species (the gallery-builder Polychaeta *Hediste diversicolor*) had an effect that was partially deviating from the general trend, being able to markedly reduce sediment resuspension at low hydrodynamic stress compared to other species. By combining this trend with hydrodynamic forces, we were able to produce a process-based model of biota-mediated sediment resuspension.

Introduction

Organisms may physically change the abiotic environment, either by their structures (*i.e.*, autogenic ecosystem engineering) or by their activity (*i.e.*, allogenic ecosystem engineering) (Jones, et al., 1994; Jones, et al., 1997). By engineering their environment, biotic agents can exacerbate or dampen ongoing physical trends (Crooks, 2002). As a noticeable case, sediment dynamics originate from the physical interaction between the drag force of the water flow and the sediment particles (Allen, 1985; Winterwerp & van Kesteren, 2004; Fagherazzi & Wiberg, 2009; Friedrichs, 2011; Zhou, et al., 2015), but they may be heavily modulated by biotic agents (Widdows & Brinsley, 2002; Le Hir, et al., 2007; Grabowski, et al., 2011; Friedrichs, 2011). Macrozoobenthos living inside the sediment are ecosystem engineers in the sense that they may alter the bottom sediment properties with their bioturbation activities (Le Hir, et al., 2007). The surface roughness generated by the bioturbators reworking the sediment may dampen the near bottom hydrodynamics and shelter the sediment surface, preventing resuspension (Friedrichs, et al., 2009; Friedrichs, 2011). Nevertheless, bioturbators generally make the sediment less resistant to erosion by loosening it with their activities (Willows, et al., 1998; Ciutat, et al., 2007; Montserrat, et al., 2008; Volkenborn, et al., 2009; van Prooijen, et al., 2011; Rakotomalala, et al., 2015; Cozzoli, et al., 2018a; Joensuu, et al., 2018). The effect of bioturbators on cohesive sediment resuspension impacts the short- and long-term development of coastal morphology (Le Hir, et al., 2007; Orvain, et al., 2012; Winterwerp, et al., 2018), and should hence be taken into account when forecasting the evolution of landscapes and ecosystems (Solan, et al., 2004; Orvain, 2005; Orvain, et al., 2012; Bouma, et al., 2014; Queirós, et al., 2015; Nasermoaddeli, et al., 2018). Beyond coastal morphology, sediment resuspension is related to the oxygenation and the transfer of particles and nutrients within the sediment layers and from the sediment surface to the water column (Ubertini, et al., 2012). For this reason, bioturbation may have a broad influence on biogeochemical cycles (Solan, et al., 2004; Quintana, et al., 2015; Thomsen, et al., 2017; Zhang, et al., 2017; Wrede, et al., 2018), pollutants diffusion (Kupryianchyk, et al., 2013) species coexistence (Mermillod-Blondin & Lemoine, 2010;

David, et al., 2016; Chen, et al., 2017) and aquatic food webs (Saint-Béat, et al., 2104; Abrantes, et al., 2014; Zou, et al., 2016).

Bioturbators are characterized by high taxonomic and functional diversity (Holtmann, et al., 1996). Five main types of functional bioturbation groups exhibiting different modes of sediment mixing may be distinguished: the biodiffusors, upward conveyors, downward conveyors, regenerators and gallery-diffusors (Lee & Swartz., 1980; Solan, et al., 2004; Queirós, et al., 2013). Species-specific trait-based models proved to have good performance in the quantitative prediction of the intensity of sediment reworking (Solan, et al., 2004; Queirós, et al., 2013; Queirós, et al., 2015) and of closely related processes as bioirrigation (Wrede, et al., 2018). However, formulating a general mechanistic framework to quantify bioturbation processes based on species-specific functional traits remains difficult due to the high variation in bioturbators' species distribution and functional behaviour, that is hardly predictable in detail (Queirós, et al., 2013). According to van Prooijen, et al. (van Prooijen, et al., 2011), widely applicable models of bio-mediated physical dynamics should be based on a set of formulations derived from generally valid (*i.e.* not site-specific or species-specific) physicochemical and biological laws, each formulation representing a (sub)process. The advantage of such process-based models is that sub-processes can be combined and results can be extrapolated, as general laws should hold everywhere.

Generalizations in ecology have often been based on body size allometries, since almost all the fundamental traits of organisms vary predictably with their size [*e.g.* (Peters, 1983; De Roos, et al., 2003; Gaston & Blackburn, 2000; Brown, et al., 2004; Marquet, et al., 2005)]. In particular, the body size of organisms shows a positive allometric relationship with their rate of biological processing of energy and material, *i.e.* the metabolic rate (Kleiber, 1932; Peters, 1983; Gaston & Blackburn, 2000; Kooijman, 2000; Brown, et al., 2004; Savage, et al., 2004; Sousa, et al., 2008). The individual metabolic rate feeds other key individual (*e.g.* development, reproduction, locomotion, oxygen and food intake), population (*e.g.* growth rate, carrying capacity), community (*e.g.* diversity, rate of interaction) and ecosystem (*e.g.* biomass production, trophic dynamics)

processes, so that it has been proposed as a holistic measure of the 'pace of life ' (Brown, et al., 2004). Ecological metabolic theories [e.g. (Brown, et al., 2004; Kooijman, 2000)] can be used to link ecological outcomes to biophysical processes by using the first principles of physics, chemistry, and biology that govern the organismic processing of energy and material.

At the individual level, the metabolic rate of bioturbators has been proposed as synthetic descriptor for the intensity of bioturbation (Cozzoli, et al., 2018a) because of its positive relation with the intensity of the physiological activities involved in the sediment bioturbation as respiration [*e.g.* burrow ventilation, valves shacking (Kristensen, 1983; Ciutat, et al., 2007)], feeding [*e.g.* swallowing, excretion and disruption of the sediment to extract organic particles (Zebe & Schiedek, 1996; van Prooijen, et al., 2011)] and moving [*e.g.* digging, crawling (Friedrichs, et al., 2009)]. Mesocosm experiments performed at constant hydrodynamic stress showed that the effect of individual bioturbation activity on sediment resuspension can be scaled to the population level (Cozzoli, et al., 2018a). This concept is also supported by the recent work of Wrede et al. (Wrede, et al., 2018), demonstrating that size scaling rules of metabolic rates can provide a base to predict the intensity of bioirrigation at community level.

With this study, we propose a process-based model [*sensu* van Prooijen et al. (van Prooijen, et al., 2011)] of bioturbators-mediated cohesive sediment resuspension. For this purpose, we explored the potential of the bioturbators' metabolic rate as a general descriptor of the biological influences on sediment resuspension in relation to changes in hydrodynamic energy, which is the main physical driver of sediment dynamics (Allen, 1985; Winterwerp & van Kesteren, 2004; Fagherazzi & Wiberg, 2009; Friedrichs, 2011; Zhou, et al., 2015). Given that: *i*) sediment reworking at the individual level usually results from the bioturbator respiration, feeding, and moving activities; *ii*) these activities are fuelled from the individual metabolic rate, of which the individual size is a proxy; *iii*) multiple individuals bioturbating the sediment cumulate their metabolic rates and their effect on sediment resuspension; we hypothesised that changes *per area* of suspended

cohesive sediment through an hydrodynamic energy gradient are fundamentally related to changes in the overall metabolic rate of the bioturbating population, rather than to specificities in the sediment reworking modality. To test the hypothesis in controlled conditions, we performed a series of mesocosm experiments by using annular recirculating flumes. To investigate if the overall activity of the bioturbating population (approximated as the population basal metabolic rate) is indeed the main driver explaining variations in the mass of suspended sediment, we compared the quantitative effect on sediment resuspension of several common species of bioturbators, characterized by different functional behaviour (Table 1).

Material & Methods

Experimental design

We used mesocosm recirculating annular flumes set-up to to mimic the environmental conditions of the intermediate - upper part of an intertidal flat (*i.e.* muddy sediment, low to intermediate hydrodynamic stress), where bioturbators are typically most abundant (Pearson & Rosenberg, 1978; Nilsson & Rosenberg, 2002) and most effective in enhancing sediment resuspension (Orvain, et al., 2012). The mesocosm approach allowed us to test the hypothesis under controlled conditions, excluding variation in both physical factors [*e.g.* sediment grain size, cohesiveness and compaction (van Prooijen & Winterwerp, 2010)], and in physiological or behavioural changes of the bioturbation activity in response to environmental cues [*e.g.* acidification (Yvon-Durocher, et al., 2012; Ong, et al., 2017); temperature (Verdelhos, et al., 2015); salinity (Verdelhos, et al., 2015); food availability (Maire, et al., 2006)]. Variations in the amount of suspended sediment (R_{TOT}, g m^{-2}) were used as a measure of the bioturbation effect on sediment erodibility along a gradient of hydrodynamic stress.

The tested combinations of bioturbator body sizes and densities were selected in a way to cover the natural range of each analysed species [*e.g.* (Zebe & Schiedek, 1996; Holtmann, et al., 1996; Degraer, et al., 2006), *i.e.* to represent from the highest densities and larger individual sizes commonly observed in nature on temperate tidal flats (therefore avoiding exceptionally high densities and large sizes) to the lowest densities and smaller sizes usable from a practical point of view, possibly including intermediate levels between extreme values. The availability of field collected and homogeneously sized experimental organisms was limited and not always sufficient to fully cover a complete factorial design, crossing all species, sizes and density levels. We did not run experiments with very high densities of large individuals (*i.e.* overall biomass > 120 g AFDW m^{-2}) due to saturation of the surface of the experimental flumes. We also avoided running experiments with very low densities of smaller individual (*i.e.* overall biomass < 0.6 g AFDW m^{-2}) because preliminary observations did not show any detectable biotic effect on sediment

resuspension below this threshold. Respecting these conditions, we managed to collect a dataset encompassing a range of bioturbators taxonomic (8 species) and functional diversity (from shallow to deep bioturbators), individual densities (13 to 6366 Ind. m^{-2}) and individual body sizes (0.25 to 1120 mg Ash Free Dry Weight, AFDW), for a total of 38 unique combinations of species, size and density plus two defaunated controls (Table 1). Each treatment always used homogeneously sized individuals of a single species and was replicated twice. The overall bioturbator population basal metabolic rates, expressed as a linear combination of individual metabolic rates at the experimental temperature and density of individuals (I_{TOT}, mW m^{-2}), were estimated for each treatment according to the empirical model for aquatic macroinvertebrates respiration of Brey (Brey, 2010) and ranged from 3 to 260 mW m^{-2} (Table 1).

A minor portion of the dataset (observations collected at bed shear stress of 0.18 Pa on a subset of species) has been published to investigate the biotic effect on sediment resuspension at a fixed current velocity in Cozzoli, et al., 2018 (Cozzoli, et al., 2018a). The complete dataset is available as Appendix of this paper (Appendix A).

Model organisms

For our measurements we used a range of bioturbators that commonly coexist on temperate muddy intertidal flats (Holtmann, et al., 1996; Degraer, et al., 2006), although with slightly different preferences for the composition of the inhabiting sediment (Anderson, 2008; Cozzoli, et al., 2013). They are all endemic of the North Atlantic Ocean with the exception of *Ruditapes philippinarum,* a non-indigenous species native of the Indian and Pacific Oceans that is rapidly expanding in the North Sea (Humphreys, et al., 2015). Cumulatively, the species accounted for in this study make up 60% of the macrozoobenthos intertidal biomass in temperate estuaries such as the Westerschelde and Oosterschelde (SW Delta, the Netherlands), and they can locally reach almost 100% (Cozzoli, et al., 2013). The model species were selected as explained below:

- Shallow-burrowing Bivalvia represented by obligatory suspension feeder *Cerastoderma edule* (Linnaeus, 1758). *C. edule* makes shallow perturbations (shells usually emerge from the sediment surface) in the sediment by crawling, shaking valves and producing pelleted pseudo-faeces, (Flach, 1996). This species can reach a relatively large individual size (up to 600 mg Ash Free Dry Weight, AFDW) and high density (adult density up to 500 Ind. m^{-2} along the North Sea coasts) (Cozzoli, et al., 2014). Several field and laboratory studies showed that *C. edule* destabilizes the cohesive sediment making it more erodible [*e.g.* (Flach, 1996; Ciutat, et al., 2007; Montserrat, et al., 2009; Li, et al., 2017)].
- Intermediate burrowing Bivalvia that live in the sediment at a depth of 3-10 cm, represented by facultative suspension feeder *Abra alba* (Wood, 1802), *Scrobicularia plana* (da Costa, 1778), *Limecola balthica* (Linnaeus, 1758) and *Ruditapes philippinarum* (Adams and Reeve, 1850). While differing in the maximal adult size [from 50 mg AFDW for *L. balthica* and *A. alba* up to 300 mg AFDW for *S. plana*, (Swartz, 1991)], these organisms share common lifestyles, and modes of feeding and mobility (Purchon, 1997; Queirós, et al., 2013), and have a similar effect on sediment resuspension (Cozzoli, et al., 2018a). They often behave as surface deposit feeders, by inhaling sediment through their siphons and

depositing pseudo-faeces (Zwarts, et al., 1994; Purchon, 1997). By doing so, they disrupt the sediment surface and increase the erodibility (Willows, et al., 1998; Widdows, et al., 1998; Orvain, 2005; Sgro, et al., 2005; van Prooijen, et al., 2011).

- Intermediate-burrowing Amphipoda that live in U-shaped burrows represented by *Corophium volutator* (Pallas, 1776). These small bioturbators (average weight 0.25 mg AFDW) may reach very high densities (up to 15000 Ind m^{-2}) in the upper part of the tidal flats (De Backer, et al., 2011). Burrows are *ca.* 5 cm deep (Flach, 1996) and their openings can protrude 1 to 1.5 mm above the sediment surface, especially in fine mud (Meadows & Reid, 1966; Meadows, et al., 1990). When acting as filter feeder, *C. volutator* pump large amounts of water through the burrows and contribute actively to sediment resuspension (De Backer, et al., 2011). If suspended phytoplankton is not abundant, surface deposit feeding is the main feeding mode, and then particles are predominantly gathered by scraping the sediment surface with the enlarged second antennae (Meadows & Reid, 1966). Its bioturbation effect on sediment stability is variable (Le Hir, et al., 2007). For instance, both negative (Meadows & Tait, 1989), positive (Gerdol & Hughes, 1994; De Backer, et al., 2011) and neutral effects (de Deckere, et al., 2000) on sediment resuspension have been observed depending upon the density of burrows and the sediment granulometry.
- Intermediate/deep-burrowing Polychaeta, that build complex gallery networks that can extend down to 30 cm depth, represented by *Hediste diversicolor* (Müller, 1776). This species may reach very high individuals densities (up to 5000 Ind. m^{-2}), especially in association with high organic load (Rasmussen, 1973; Abrantes, et al., 1999). *H. diversicolor* are omnivores and detritivores that feed by swallowing surface sediments around the burrow opening. The burying depth is positively related to body length, although individuals longer than10 cm can be commonly found in the upper 2–3 cm (Fernandes, et al., 2006). *H. diversicolor* are known to create extensive gallery networks that they actively ventilate, increasing the flux of oxygen and nutrients over the sediment–water interface

(Kristensen, 1983; Kristensen, 2001; Hedman, et al., 2011; Zhu, et al., 2016) The movements *of H. diversicolor* in the the gallery network generate particles mixing in the surficial sediment layers and an accumulation of particles in the bottom layers due to non-local transport (Duport, et al., 2006; Hedman, et al., 2011). This species is considered by some authors as a stabiliser because it enhances stability by lateral compaction of the sediment around the burrows (Meadows & Tait, 1989; Meadows, et al., 1990) and damp the hydrodynamic stress by the creation of skimming flow by protruding galleries (Friedrichs, 2011). Other authors have instead highlighted that *H. diversicolor*, while being able to increase the sediment resistance to initial motion, have a positive effect on sediment resuspension when the hydrodynamic stress increases (Fernandes, et al., 2006).

- Deep-burrowing Polychaeta that live generally more than 10 cm deep in the sediment in J-shaped burrows, represented by *Arenicola marina* (Linnaeus, 1758). *A. marina* are large worms (up to 2 g AFDW) that swallow surface sediment through a feeding funnel and expel it in the form of pseudo-faeces, forming characteristic feeding pits and pseudo-faeces casts, (Zebe & Schiedek, 1996; Volkenborn, et al., 2009). They are typically found in North European intertidal flats in densities of up to 100 individuals m^{-2} (Beukema & de Vlas, 1979). The sediment reworking from *A. marina* feeding activity increases the sediment volume exposed to hydrodynamic forcing and dramatically increase the resuspension of fine particles (Volkenborn, et al., 2009; Wendelboe, et al., 2013).

Considering the large number of flume runs needed, the time-consuming character of each flume experiment and the fact the bioturbators may exhibit seasonal variation in their behaviour, the experiments were performed during spring in two annual tranches. Animals were collected between April - June 2011 and between April - June 2012 from the intertidal flats of the Oosterschelde and Westerschelde. The species involved in this study are not endangered or protected. The authorization for specimen collection was issued by the competent authority Rijkswaterstaat. The

mortality during experiment was generally very low and the animals were released at the collection site at the end of the experiments.

To avoid confounding effect related to temperature variation, all experiments were performed at a constant temperature of 18 °C, *i.e.* the average water temperature in the Westerschelde and Oosterschelde during full summer. We chose this temperature because, due to the positive relationship between ectotherms' metabolic rates and temperature (Pörtner & Farrell, 2008), it is the one at which bioturbators should be more active within their natural temperature range. At the time of collection, average daily water temperature was between 14 and 17 °C. After collection, the bioturbators were always allowed to acclimate for 1 week in containers filled with sediment and aerated filtered marine water that was kept at 18 °C. Considering the relatively limited difference in temperature between field and mesocosms, one week of acclimation (rather than the two weeks usually adopted in macrozoobenthos studies) should be sufficient to reduce the risk of temperature shock that could severely affect bioturbator metabolic rates (Nascimento, et al., 1996). During the acclimation period the bioturbators have been fed with liquid algal extract or fish food. Experiments were performed directly after this week of acclimation.

Bioturbators' individual body mass (mg Ash Free Dry Weight, AFDW) was estimated from the individual length (mm, bivalves) or wet weight (mg, *A. marina*, *H. diversicolor*, *C. volutator*), according to the relationships provided from the NIOZ – Yerseke Monitor Taskforce. Bioturbators' individual metabolic rates were estimated according to the empirical model for aquatic macroinvertebrates respiration of Brey (Brey, 2010) assuming an average energy density of 21.5 J mg^{-1} (Brey, 2001) and an operational temperature of 18 °C and using a trait classification for sessile (bivalves, *A. marina*) or motile (*C. volutator* and *H. diversicolor*) intertidal satiate Anellida, Artropoda or Bivalvia Heterodonta. The overall bioturbators population metabolic rate (I_{TOT}, mW m^{-2}) was estimated as the product of the individual metabolic rate and the population density (Allen, et al., 2005).

Experimental devices

The recirculating annular flumes we used follow the design described by (Widdows, et al., 1998; Cozzoli, et al., 2018a). The annular channel has a surface of 157 cm^2. In the majority of the cases, we used flumes with an overall height of 40 cm, of which the bottom 5 cm are filled with a pebbled bed to allow water drainage, followed by 10 cm of consolidated sediment and 20 cm of filtered marine seawater (31.4 L). A modified version with an overall height of 80 cm and a sediment column of 50 cm was used to allow the largest sized *A. marina* to settle properly.

The muddy sediment used in this experiment (median grain size 120 µm, silt content 12% measured by using a Malvern Mastersizer 2000® particle analyser) was collected in late winter 2011 at location Zandkreek Dam (51°32'N, 3°52'E) in the Oosterschelde. The sediment was carefully sieved over a 1 mm sieve to avoid the presence of large particles (stones, shells, wooden pieces) and to remove large macrozoobenthos. Successively, it was covered with a thick black plastic film for at least two weeks to kill remaining benthos and sieved again. As such, all macrozoobenthos was removed from the sediment. One week before of the experiments, the wet sediment was aerated and put in a flume, mixed to a smooth mass and allowed to consolidate. Although shorter than the time the sediment takes to return to a realistic porewater gradient after a big disturbance [13 days according to Porter, et al. 2006 (Porter, et al., 2006)], preliminary observations showed that a one week consolidation time is sufficient to obtain a firm and homogeneous bottom between treatments.

The water motion in the annular flumes was generated by a smooth disk rotating 3 cm below the water surface, which was driven by a microprocessor-controlled engine. An acoustic Doppler velocimetry probe was used to calibrate water flow velocity as a function of engine rotation speed. The hydrodynamic Bed Shear Stress (BSS, Pa) was estimated from the depth-average water flow velocity v (m sec^{-1}) as:

$$BSS = \rho f v^2 \qquad \text{Eq. 1}$$

where ρ is the density of marine water (1024 kg m^{-3}) and f is a constant friction factor, i.e. 0.002 (Roberts, et al., 2000). We deliberately assign a constant f to exclude from equation 1 the possible influence of bioturbations on sediment surface friction. The friction of disrupted sediment surface will thus be considered as property of the specimens and included in the bioturbation effect.

Water turbidity, as a proxy of suspended sediment, is measured using an optical backscatter sensor (OBS 3+, Campbell scientific) facing the water perpendicularly to the current direction at 10 cm from the sediment surface and measuring the water turbidity every 30 sec. The effect of the suspended sediment on light absorption was measured by the OBS sensors and converted into Suspended Sediment Concentration (SSC, g L^{-1}) based on calibration by gravitometric analysis [(Cozzoli, et al., 2018a)]. The SSC in the water is coupled with the mass of bottom sediment by a dynamic balance between deposition and erosion. Increasing bottom shear stress has the effect to increase the sediment erosion and decrease the sediment deposition, thus increasing the SSC. Analogously to previous studies [*e.g.* (Willows, et al., 1998; van Prooijen, et al., 2011)], we did not measure sediment deposition and we only consider the effect of bioturbation on the equilibrium SSC reached at a given level of bed shear stress from water motion (i.e., deposition rate = erosion rate, so that the suspended sediment concentration is constant). Previous studies (Willows, et al., 1998; Ciutat, et al., 2007; Li, et al., 2017) have shown that, for this kind of experiments, supply-limited erosion mostly occurs. That is, after the water motion has started, the SSC reaches equilibrium due to limitation of erodible material (Mehta & Partheniades, 1982; van Prooijen & Winterwerp, 2010). In our experiments, the equilibrium SSC was usually reached after ca. 5 minutes of applying current. To express sediment resuspension in spatial units, we converted the SSC to total mass of suspended sediment per unit of sediment surface present in the flume (R_{TOT}. g m^{-2}).

Experimental procedures

To simulate the natural dynamic changes in current velocity during the flood tide on a shallow flat, we increased the current in the experimental flumes from 10 cm sec^{-1} (Bed Shear Stress of 0.05 Pa) to 30 cm sec^{-1} (BSS of 0.25 Pa) by steps of 5 cm sec^{-1}, each step lasting 20 minutes. To determine the mass of suspended sediment per unit of sediment surface (R_{TOT}. g m^{-2}) at each step of current velocity, we considered the average of the measurement collected in the last 2.5 minutes of the step, when the supply-limited suspended sediment concentration was quasi-stable.

The bottom sediment was smoothed before each replicate by running the flume without any bioturbator inside. As a consequence of the limited erosion that occurred during this procedure, a uniform, less than 0.5 mm-thick layer of fine sediment was deposited on the sediment surface of each flume within a few hours from the end of the run. Pilot experiments conducted in flumes without fauna, involving several sequential daily runs, showed some small differences across flumes, but no increase in sediment resuspension compared to the smoothing procedure.

After smoothing the bottom, bioturbators were evenly distributed over the sediment surface and allowed to settle for 48 h. The choice of a longer time interval (48 h) compared with the typical interval between erosion stress peaks (typically 12 or 24 h in a tidal system) was necessary to give the animals the time to properly settle in the new environment and recover from manipulation stress. The vast majority of them were buried within a few minutes after being placed in the flume and non-burrowing individuals were replaced. During their presence in the flume, some bivalves (especially *C. edule*) crawled on and below the sediment surface, leaving evident tracks. The intermediate burrowers bivalves left evident siphoning tracks around their burying site. Few *C. volutator* were swimming or crawling over the surface at a time, while the large majority was buried. *H. diversicolor* released mucus and faeces on the sediment surface while burying themselves and developed a system of galleries from which they rarely fully emerged. *A. marina* generally did not move from the initial settlement point and produced a single feeding pit with a pseudo-faeces cast for each individual.

Data analysis

Assuming supply-limited sediment erosion (Mehta & Partheniades, 1982; van Prooijen & Winterwerp, 2010), the relationship between the the mass of suspended sediment per unit of sediment surface (R_{TOT}. g m^{-2}) reached at each current velocity step and the applied hydrodynamic Bed Shear Stress (BSS, Pa) was modelled as a logistic sigmoidal curve:

$$R_{TOT} = \frac{a}{1+e^{\frac{b-BSS}{c}}} \qquad \text{Eq. 2}$$

where the coefficient *a* is the maximal expected value of R_{TOT} (asymptote of the erosion curve, g m^{-2}), the coefficient *b* is the BSS value at which 50% of the value of *a* is reached (midterm of the erosion curve, Pa) and *c* is a scale coefficient that allows accounting for the steepness of the curve at the inflection point. By analysing the data *via* non-linear mixed modelling (Bolker, et al., 2009; Zuur, et al., 2009), we allowed for random variations in the coefficients *a* and *b* across the full combination of bioturbators species, density and size gradients (Table 1).

Systematic variations in the asymptote *a* and the midterm *b* across the different treatments were analysed *via* linear ANCOVA. A multivariate regression model of each of the coefficients *a* and *b* was fitted using the bioturbators species as categorical variable and four basic descriptors of the investigated population as continuous variables: individual size (*M*, mg AFDW), density of individuals (*D*, N of Ind. m^{-2}), total biomass (M_{TOT} mg AFDW m^{-2}) and overall population metabolic rate (I_{TOT}, mW m^{-2}). To match the linear ANCOVA assumptions, the asymptote *a* distribution was normalized *via* log transformation and the distribution of the variables individual size, density of individuals, total biomass and I_{TOT} was normalized *via* log plus 1 transformation. The best predictors were selected by AIC comparison and elimination stepwise procedure. The relative importance of the predictors in explaining variance was assessed by LMG metrics [R^2 partitioned by averaging over orders (Lindeman, et al., 1980)]. All analyses were performed within the free software environment R 3.3.2 (R-Core-Team, 2017) using the lmer (Bates, et al., 2015) and relaimpo (Grömping, 2006) packages.

Results

All the tests show that mass of suspended sediment per unit of sediment surface (R_{TOT}. g m^{-2}) increases consistently with the Bed Shear Stress (BSS, Pa). The highest R_{TOT} recorded in the defaunated controls was 40.02 g m^{-2} at the maximal BSS of 0.25 Pa. Values of R_{TOT} higher than 150 g m^{-2} were recorded in presence of bioturbators due to general failures of the flume bed and consequent mass erosion. These values were not accounted for in the analysis. After this skimming, the highest recorded R_{TOT} was 133 g m^{-2} for *S. plana* (large individuals) at BSS of 0.18 Pa. A slight decrease in R_{TOT} was observed at low BSS and low densities of bioturbators (Figure 1). Exceptional behaviour was shown by *H. diversicolor*, which are able to considerably decrease R_{TOT} up to a BSS of 0.20 Pa at each tested density of individuals.

A logistic sigmodal function of the BSS (Equation 2) was able to explain 53 % of the marginal variance of R_{TOT} (*i.e.* that part of variance of R_{TOT} attributable to the fixed factor BSS) Accounting for random variations in the asymptote *a* and the midterm *b* for each treatment, 97% of the conditional variance of R_{TOT} (*i.e.* that part of variance of R_{TOT} attributable to both the fixed factor BSS and the random variation across treatments) was explained (Figure 1, Table 2).

The presence of bioturbators have the effect to increase both the maximal (asymptotic) amount of eroded sediment (coefficient *a* in Equation 2) and the hydrodynamic energy needed to reach the midterm of the erosion curve (coefficient *b* in Equation 2) (Table 1).

As a single descriptor, the overall population metabolic rate of the bioturbators (I_{TOT}, mW m^{-2}) is able to explain most of the variance (54 %) in the asymptote *a* (Table 3) with better performance than the other descriptors considered (*i.e.* Individual Size, Density of Individuals and overall Biomass; Appendix B, Table B1) [± 95% CI]:

$$a_{BIO}=40.45[\pm 9.95]*(1+I_{TOT})^{0.24[\pm 0.07]} \qquad \text{Eq. 3.1}$$

In association with other descriptors, the individual size of the bioturbators (*M*, mg AFDW) have also been selected *via* stepwise procedure as significant explanatory variable. The negative relationship with *M* contributes to explain a further 8 % of variance in a_{BIO} (Table 3):

$$a_{BIO}=41.67[\pm 9.07]*(1+I_{TOT})^{0.34[\pm 0.12]}*(1+M)^{-0.09[\pm 0.06]} \qquad \text{Eq. 3.2}$$

The stepwise variable selection excludes significant interspecific variations of a_{BIO} (Table 3).

I_{TOT} is also a significant descriptor of the midterm b of the erosion curve, despite being able to explain a smaller amount of variance (20%) than it does for the asymptote a_{BIO} (Table 4):

$$b_{BIO}=0.1[\pm 0.04]+0.02[\pm 0.01]*log(1+I_{TOT}) \qquad \text{Eq. 4.1}$$

As a single population descriptor, the metabolic rate has a performance comparable to the total biomass and higher than that of the individual size or density of individuals in describing the variance of b_{BIO} (Appendix B, Table B2). Differently from the asymptote a_{BIO}, the midterm b_{BIO} is subject to significant interspecific variations, to which 50% of the observed variance can be attributed (Table 4):

$$b_{BIO}=0.1[\pm 0.03]+0.01[\pm 0.009]*log(1+I_{TOT})+Species \qquad \text{Eq. 4.2}$$

The interspecific variability of b_{BIO} is mostly related to the effect of *H. diversicolor*, the only species for which we observed a strongly significant ($p < 0.001$) higher b value than for other species (Table 1, Table 4).

In all cases, the intercepts of the scaling models (*i.e.* condition of absence of bioturbators) match the values of a and b estimated for defaunated controls, indicating that the models are compatible with a physical description of the relationship between BSS and cohesive sediment resuspension (Table 3, Table 4).

From Equations 3.1 and 4.1 it follows that R_{TOT} may be predicted as a function of the combination of BSS and I_{TOT} by replacing in Equation 2 the parameter a by a_{BIO} and replacing b by b_{BIO}:

$$R_{TOT} = \frac{a_{BIO}}{1+e^{\frac{b_{BIO}-BSS}{c}}} \qquad \text{Eq. 5}$$

Equation 5 is able to explain 62 % of the variance in the observed R_{TOT} values, with a ratio between observed and predicted values very close to 1:1 (Figure 3, Table 5). Including the negative dependence of a_{BIO} from the individual size (Equation 3.b), the variance in the observed R_{TOT} values

explained by Equation 5 rises to 64% and reaches 78 % if the interspecific variations of the midterm (Equation 4.b) are considered (Figure 3, Table 5). This means that a heterogeneous process such as sediment resuspension induced by bioturbators with different functional characteristics can be effectively described as a function of I_{TOT} and BSS, accounting for some differences for bioturbators species with different functional characteristics as *H. diversicolor*.

Discussion

In this paper, we derive a unified view of bioturbation effects on supply-limited resuspension of cohesive sediment and a general relationship to quantify such effect along a hydrodynamic stress gradient (Equation 5). Equation 5 provides a description of a physical trend (relationship between Bed Shear Stress and cohesive sediment supply-limited erosion, shaped as a sigmoidal curve) in which the physical constants (the asymptote *a* and the midterm *b*) are replaced by empirical descriptions of the behaviour of organisms (a_{BIO} and b_{BIO}). It meets the requirements indicated by van Prooijen, et al. (van Prooijen, et al., 2011) for process-based models of bio-mediated physical dynamics in the sense that: *i*) it is composed of a set of formulations representing sub-processes (*i.e.* the physical effect of Bed Shear Stress on cohesive sediment resuspension; the effect of bioturbators on the amount of sediment suspended at different BSS) *ii*) it is mainly based on general ecological principles of size and energy scaling that should hold for any organism, although with some specific variation in the parameters *iii*) it is fully compatible with a physical description of the processes in case of no biogenic influences, as the intercepts of the scaling models for the coefficients a_{BIO} and b_{BIO} match the values predicted for the defanauted control; *iv*) it is affected by a minimum number of physically well-defined parameters (mainly BSS and energy use rate of the bioturbators, in this study case). Being a process based model, Equation 5 has the potential to be further developed to include additional processes generating variance in a_{BIO} and b_{BIO} (*e.g.* different typologies of sediment, different typologies of ecosystem engineers). It must be however considered that, in its present form, Equation 5 concerns supply-limited erosion only (Mehta & Partheniades, 1982; van Prooijen & Winterwerp, 2010). At a BSS higher than the maximal we tested, mass erosion may overcome the importance of bioturbation in determining sediment resuspension.

Within the range of tested conditions, random variations across treatments with different bioturbator species, size and density were as important as the fixed effect of hydraulic Bed Shear Stress (BSS) in explaining variations in the mass of suspended sediment. Different population

descriptors such as the individual size, the density of individuals or the total biomass may be used as proxy for the bioturbators effect on sediment resuspension. The metabolic rate is a more general index which encompasses these multiple parameters, and it has the advantage of being mechanistically related to the organisms' bioturbation activity, rather than being a proxy of it. Variations in a_{BIO} and b_{BIO} can be efficiently described in terms of overall bioturbators population metabolic rate, although descriptions of the individual size (a_{BIO}) and species-specificities (b_{BIO}) of bioturbators may contribute in improving the accuracy of Equation 5.

Effect of bioturbator metabolism on the amount of suspended sediment at high BSS

The most important biological driver for amount of destabilized and suspended sediment at high BSS is the overall bioturbators population metabolic rate, which explains 56% of the cross-treatment variation in the asymptote of the erosion curve (coefficient a_{BIO} in Equation 5). This is related to the fact that the bioturbators' activities are able to disrupt cohesiveness and compaction in the upper layers of sediment, generating a fluff layer that starts to be suspended from a BSS of *ca.* 0.15 Pa (Orvain, et al., 2003; van Prooijen, et al., 2011). Our measurements show that the overall amount of sediment contained in the fluff layer is proportional to the activity (approximated as population basal metabolic rate) of the bioturbators inhabiting the sediment.

A minor but significant variant component of the coefficient a_{BIO} (8 %) is explained by a negative relationship with individual body size. A potential interpretation for this trend is that smaller individuals dig less deeply (Zwarts & Wanink, 1989; Zebe & Schiedek, 1996; Fernandes, et al., 2006), causing them to use their energy to rework more surficial and exposed sediment. It is also possible that smaller individuals could represent earlier life stages, characterized by higher metabolic rates (Glazier, 2005; Glazier, et al., 2011) than what we have estimated from the empirical model of Brey (Brey, 2010).

Effect of bioturbators metabolism on the amount of suspended sediment at low BSS

The presence of bioturbators have the effect to increase the hydrodynamic energy needed to reach the midterm of the erosion logistic curve (b_{BIO} in Equation 5). Species-specific differences have a major importance in determining the value of b_{BIO}. Together with specific variations, we observed a positive relationship between b_{BIO} and the overall bioturbators population metabolic rate. This indicates that at high levels of bioturbation activity, a proportionally lower amount of sediment is suspended at low BSS. This pattern is possibly related to the fact that bioturbators are able to shelter the sediment surface from shear flow when the hydrodynamic forcing is low (Friedrichs, et al., 2009; Friedrichs, 2011). The reworking by the animals could also change the structure of the sediment: excreted sediments can be pelletized and compacted, becoming slightly more resistant to initial erosion (Briggs, et al., 2015). The positive dependence of the midterm b_{BIO} on population metabolism may be explained by considering that these processes (changes in microtopography of the sediment surface, pelletization of the sediment) are also products of the bioturbators' activity and metabolism, hence they should scale positively with the individual size and density of individuals. However, bioturbation led only to a minor reduction in suspended sediment at low BSS, that is suppressed at higher BSS by the opposite destabilizing effect.

Effect of different types of bioturbators

We observed that differences in bioturbators species and functional behaviour do not have a significant influence on the (asymptotic) amount of sediment suspended at high BSS (a_{BIO}). Instead, the midterm of the erosion logistic curve (b_{BIO}) varies across species, mostly in relation to the effect of the gallery-builder *H. diversicolor*. Compared to other species, *H. diversicolor* markedly reduce sediment resuspension at low BSS (< 0.2 Pa). This observation could outline a stabilizing effect of this species, that is likely related to the lateral compaction of the gallery walls during burrowing activity and to the secretion of mucus that is pushed against the walls, both consolidating the burrows and increasing the cohesiveness of the sediment (Meadows & Tait, 1989; Meadows, et al., 1990; Fernandes, et al., 2006). Considering that *H. diversicolor* also displaces surface particles down to the gallery bottom (Duport, et al., 2006; Hedman, et al., 2011), dissolve the internal pool of particulate nutrients in the sediment (Ieno, et al., 2006; Hedman, et al., 2011) and contribute to seed burial (Zhu, et al., 2016) it is possible that this species, at BSS and individual densities comparable to what we tested, may promote the compaction of the recently deposited sediment and the accretion of tidal flats and marshes. However, the sediment stabilizing effect of *H. diversicolor* is limited to low shear stress. When the BSS reaches and exceeds 0.20 Pa, *H. diversicolor* have an effect similar to the other bioturbators, confirming what was earlier reported by previous studies (Fernandes, et al., 2006; Widdows, et al., 2009). Also, at higher densities of individuals (3000 Ind. m^{-2}) than what we tested in our experiments (318-955 Ind. m^{-2}) *H. diversicolor* have been observed to increase sediment resuspension even at low hydrodynamic stress (Widdows, et al., 2009).

Our measurements were focused on single species and homogeneous size experiments in order to emphasize scaling relationships. The effects of individual species on sediment resuspension in a mixed benthic community may be rather complex, depending on how interspecific interactions affect the activity of the involved species; these must also be accounted for in order to extrapolate mesocosm observations to field contexts (Orvain, et al., 2012; Kristensen, et al., 2013). A particularly important interaction to be accounted for in field conditions is that one with

biostabilizers (*i.e.* organisms that are able to enhance the sediment resistance to erosion). As an example, the microphytobenthos, that is also abundant in the upper part of intertidal flats, can produce sticky extracellular polymeric substances (Vos, et al., 1998) able to increase sediment resistance to erosion (Sutherland & Grant, 1998; Tolhurst, et al., 2006). On the one hand, by disrupting and grazing the diatom film, benthic bioturbators may have a much higher relative impact on mudflat morphology than what we measured in our flumes because they are able to trigger the resuspension of sediment that is otherwise stabilised by diatoms (Montserrat, et al., 2008), *i.e.* even more resistant to erosion than our sediment controls free of phytobenthos. On the other hand, bioturbators may promote the microphytobenthos growth by organically enriching the sediment [*i.e.* (Andersen, et al., 2010; Donadi, et al., 2013)]. As another example, biostabilizers such as sessile tube-builder worms (*e.g. Lanice conchilega*), reef forming bivalves (*e.g.* mussels, oysters) and riparian plants (*e.g. Spartina anglica, Phragmites australis*) occur in dense reefs, tussocks or canopies that exclude bioturbators inside them. However, they can modify the hydrodynamics and the sedimentary landscape around their aggregates, affecting the conditions relevant to determine the bioturbators community size/density structure (Walles, et al., 2015). In turn, sediment destabilization and seed predation from bioturbators may affect the establishment of biostabilizers (van Wesenbeeck, et al., 2007; Suykerbuyk, et al., 2012; Zhu, et al., 2016). The interplay between biostabilizers and biodestabilizers needs to be taken into account for a more complete understanding of the biotic influences of sediment resuspension.

Being mostly based on general size scaling laws, Equation 5 has the potential to be applied to describe the effect of a broader size and functional range of ecosystem engineers than what we tested in our experiment. As an example, it could be adapted to describe the effect of biodepositors (*i.e.* organisms that with their activity or presence establish a positive net flux of particles from the water column to the bottom, *e.g.* filtrators) and biostabilizers (i.e. organisms that with their activity and presence make the sediment more resistant to erosion) on sediment resuspension by allowing negative metabolic dependence of the asymptote a_{BIO} and stronger positive metabolic dependence

of the midterm b_{BIO}. For organisms influencing the sediment dynamics mainly by their presence rather than activity, the overall biovolume may be a more appropriate descriptor of their effect on sediment resuspension than I_{TOT}.

Application potential

Ecological theory that is grounded in metabolic currencies and constraints offers the potential to link ecological outcomes to biophysical processes across multiple scales of organization (Humphries & McCann, 2014). Descriptions of ecosystem engineering have a particular relevance in predicting changes in landscape evolution (Pearce, 2011). Process-based models of bioturbation effects as those we presented may contribute to the prediction of both long and short-term morphodynamic trends (Hu, et al., 2015; Hu, et al., 2018) also as response to human modifications of coastal landscapes (Cozzoli, et al., 2017; Valdemarsen, et al., 2018). Having such a metabolism-based relationship does enable extrapolations on how change in benthic community metabolism may influence bioturbation effects on sediment resuspension.

Formulations describing the field distribution of bioturbators metabolic rates with respect to environmental conditions may be included in Equation 5 as sub-processes. For local applications, the metabolic rate of bioturbator communities (and therefore their potential contribution to sediment resuspension) can be estimated with good approximation from field surveys, or they can be predicted by using empirical models relating average size and density of benthic communities to the environmental conditions in which they occur [*e.g.* (Cozzoli, et al., 2017; Gjoni, et al., 2017; Gjoni & Basset, 2018)], in association with empirical models of metabolic rates of benthic invertebrates [*e.g.* (Brey, 2010)]. About this point, it is important to consider that the hydrodynamic stress is a main driver of realized macrozoobenthic community composition and size structure [*e.g.* (Ysebaert & Herman, 2002; Thrush, et al., 2005; Cozzoli, et al., 2017)]. This implies that both the spatial distribution of bioturbators and the combined effect of hydrodynamic stress and bioturbators on sediment resuspension and can be fundamentally predicted by the same prognostic hydrodynamic model. Remote sensing of primary production [*e.g.* (Daggers, et al., 2018)] and carbon fluxes [*e.g.* (Brock, et al., 2006)] and models of energy flow across trophic levels [*e.g.* (van der Meer, et al., 2013)] may be used to estimate the metabolic rate of benthic communities from satellite observations.

Beyond size, metabolic rates of ectotherms are strongly dependent on the environmental temperature according to a positive Boltzmann-Arrhenius relationship (Clark & Johnston, 1999; Gillooly, et al., 2001; Ernest, et al., 2003; Gillooly, et al., 2006; Clarck, 2006; Pörtner & Farrell, 2008). Accounting for the effect of temperature into metabolic – mediated sediment resuspension models may help explaining seasonal variations in biotic contribution to sediment transport (Cozzoli, et al., 2018a; Wrede, et al., 2018). To more broadly predict and compare the biotic contribution to sediment resuspension across different ecosystems, general allometric theories of scaling of metabolic rates with temperature, individual size and population density [*e.g.* (Damuth, 1991; Kooijman, 2000; Brown, et al., 2004; Brown, et al., 2007)] may be joined to general models of benthic community structure in streams and transitional waters [*e.g.* (Vannote, et al., 1980; Pearson & Rosenberg, 1978; Guelorget & Perthuisot, 1992; Tagliapietra, et al., 2012)].

Conclusion

With this study, we developed a unified view and general approach to scale the effects of bioturbation on sediment erodibility along a hydrodynamic stress gradient. We showed that the effect of bioturbators on cohesive sediment resuspension can be described by bioturbators' population metabolic rate, with minor variations across different bioturbation modalities. This finding is in-line with other studies showing that indicators based on community size structure, rather than on species-specific characteristics, can be used to describe functional ecological processes or patterns such as community interactions (McGill, et al., 2006) and structure (Gjoni, et al., 2017; Gjoni & Basset, 2018), resource exploitation (Basset, et al., 2012a; Cozzoli, et al., 2018b; Cozzoli, et al., 2019), species coexistence (Canavero, et al., 2014), habitat carrying capacity (Edgar, 1993) and ecological status (Mouillot, et al., 2006; Menezes, et al., 2010; Basset, et al., 2012b). This is important as it allows to place empirical observations of biota-sediment interactions in the broader frame of general energetic theories [*e.g.* (Kooijman, 2000; Brown, et al., 2004)], establishing a link between the metabolic rates of individuals and the ecological roles of organisms in geomorphology and landscape evolution.

Acknowledgments

We gratefully thank the following people and companies: Conrad Pilditch for providing insights on the flumes realization; Jansen Tholen B.V. for the flumes realization, Lowie Haazen, Bert Sinke, Jos van Soelen for their fundamental technical support and for their patience; Nilmawati, for her contribution during the experiments; three anonymous reviewers for their insightful comments that greatly contribute to the improvement of this paper. This work was funded by the Ecoshape/Building with Nature project, with the contribution of the CoE-Oesterdam project. At the time of starting this project, NIOZ-Yerseke belonged to the Netherlands Institute of Ecology.

Bibliography

Abrantes, A., Pinto, F. & Moreira, M., 1999. Ecology of the polychaete Nereis diversicolor in the Canal de Mira (Ria de Aveiro, Portugal): population dynamics, production and oogenic cycle. *Acta Oecol. ,* 20(4), p. 267–283.

Abrantes, K. G., Barnett, A. & Bouillon, S., 2014. Stable isotope-based community metrics as a tool to identify patterns in food web structure in east African estuaries. *Funct. Ecol.,* Volume 85, p. 270–282.

Allen, A., Gillooly, J. & Brown, J., 2005. Linking the global carbon cycle to individual metabolism. *Funct Ecol.,* Volume 19, pp. 202-213.

Allen, J., 1985. Field measurement of longshore sediment transport sandy hook, New Jersey, USA. *Journal of Coastal Research,* Volume 1, p. 231–240.

Allgeier, J. et al., 2015. Metabolic theory and taxonomic identity predict nutrient recycling in a diverse food web. *Proceedings of the National Academy of Science,* Issue 112.

Andersen, T. et al., 2010. Erodibility of a mixed mudflat dominated by microphytobenthos and Cerastoderma edule, East Frisian Wadden Sea, Germany. *Est. Coast. Shelf Sci.,* Volume 87, pp. 197-206.

Anderson, M., 2008. Animal-sediment relationships re-visited: Characterising species' distributions along an environmental gradient using canonical analysis and quantile regression splines. *J Exp Mar Biol Ecol,* Volume 366, p. 16−27.

Basset, A. et al., 2012b. A benthic macroinvertebrate size spectra index for implementing the Water Framework Directive in coastal lagoons in Mediterranean and Black Sea ecoregions. *Ecol. Ind.,* 12(1), pp. 72-83.

Basset, A., Cozzoli, F. & Paparella, F., 2012a. A unifying approach to allometric scaling of resource ingestion rates under limiting conditions. *Ecosphere,* Volume 3, p. 2.

Bates, D., Maechler, M., Bolker, S. & Walker, S., 2015. Fitting linear mixed-effects models using lme4. *Journal of Statistical Software,* Volume 67, pp. 1-48.

Beukema, J. & de Vlas, J., 1979. Population parameters of the lugworm, Arenicola marina, living on tidal flats in the Dutch Wadden Sea. *Neth. J. Sea Res. ,* Volume 13, pp. 331-353.

Bolker, B. et al., 2009. Generalized linear mixed models: a practical guide for ecology and evolution. *Trends Ecol. Evol.,* Volume 24, pp. 127-135.

Bouma, T. et al., 2014. Identifying knowledge gaps hampering application of intertidal habitats in coastal protection: Opportunities & steps to take. *Coast. Eng.,* Volume 87, pp. 147-157.

Brey, T., 2001. *Population dynamics in benthic invertebrates.* [Online]
Available at: http://www.thomas-brey.de/science/

Brey, T., 2010. An empirical model for estimating aquatic invertebrate respiration. *Methods Ecol. Evol.,* Volume 1, p. 92–101.

Briggs, K., Cartwright, G., Friedrichs, C. & Shivarudruppa, S., 2015. Biogenic effects on cohesive sediment erodibility resulting from recurring seasonal hypoxia on the Louisiana shelf. *Cont. Shelf Res.,* Volume 93, pp. 17-26.

Brock, J. et al., 2006. Northern Florida reef tract benthic metabolism scaled by remote sensing. *Mar. Ecol. Prog. Ser.,* Volume 312, pp. 123-139.

Brown, J., Allen, A. & Gillooly, J., 2007. The metabolic theory of ecology and the role of body size in marine and freshwater ecosystems. In: *Body size: the structure and function of aquatic ecosystems.* Cambrige: Cambridge University Press, pp. 1-15.

Brown, J. et al., 2004. Toward a metabolic theory of Ecology. *Ecology,* Volume 82, p. 1771–1789.

Canavero, A., Hernández, D., Zarucki, M. & Arim, A., 2014. Patterns of co-occurrences in a killifish metacommunity are more related with body size than with species identity. *Austr. Ecol.,* Volume 39, pp. 455-461.
Chen, X. et al., 2017. Bioturbation as a key driver behind the dominance of Bacteria over Archaea in near-surface sediment. *Sci. Rep.,* Volume 7.
Ciutat, A., Widdows, J. & Pope, N., 2007. Effect of Cerastoderma edule density on near-bed hydrodynamics and stability of cohesive muddy sediments. *J. Exp. Mar. Bio. Ecol.,* 346(1–2), pp. 114-126.
Clarck, A., 2006. Temperature and the metabolic theory of ecology. *Funct. Ecol.,* Volume 20, pp. 405-412.
Clark, A. & Johnston, N., 1999. Scaling of metabolic rate with body mass and temperature in teleost fish. *J. Anim. Ecol.,* Volume 68, p. 893–905.
Cozzoli, F. et al., 2018a. The combined in uence of body size and density on cohesive sediment resuspension by bioturbators. *Sci. Rep.,* 12.8(3831).
Cozzoli, F., Bouma, T., Ysebaert, T. & Herman, P., 2013. Application of non-linear quantile regression to macrozoobenthic species distribution modelling: comparing two contrasting basins. *Mar. Ecol. Prog. Ser.,* Volume 475, pp. 119-133.
Cozzoli, F. et al., 2014. A mixed modeling approach to predict the effect of environmental modification on species distributions. *Plos One,* Volume 9, p. e89131.
Cozzoli, F., Gjoni, V. & Basset, A., 2019. Size dependece of patch departure behavior: evidence from granivorous rodents. *Ecology,* Volume In press.
Cozzoli, F., Ligetta, G., Vignes, F. & Basset, A., 2018b. Revisiting GUD: an empirical test on size-dependencies of patch exploitation behaviour. *PLoS One,* 13(9), p. e0204448.
Cozzoli, F. et al., 2017. A modeling approach to assess coastal management effects on benthic habitat quality: A case study on coastal defense and navigability. *Estuar. Coast. Shelf S.,* Volume 184, pp. 67-82.
Crooks, J., 2002. Characterizing ecosystem-level consequences of biological invasions: the role of ecosystem engineers. *Oikos,* Volume 97, p. 153–166.
Daggers, T., Kromkamp, J., Herman, P. & Van Der Wal, D., 2018. A model to assess microphytobenthic primary production in tidal systems using satellite remote sensing. *Remote Sens. Environ.,* Volume 211, pp. 129-145.
Damuth, J., 1991. Ecology - Of size and abundance. *Nature,* Volume 351, p. 268–269.
David, V. et al., 2016. Impact of biofilm resuspension on mesozooplankton in a shallow coastal ecosystem characterized by a bare intertidal mudflat. *J. Mar. Biol. Assoc. UK,* Volume 96, p. 1319–1329.
De Backer, A. et al., 2011. Bioturbation effects of Corophium volutator: Importance of density and behavioural activity. *East. Coast. Shelf Sci.,* Volume 91, pp. 306-313.
de Deckere, E., van de Koppel, J. & Heip, C., 2000. The influence of Corophium volutator abundance on resuspension. *Hydrobiologia ,* Volume 426, pp. 37-42.
De Roos, A., Persson, L. & McCauley, E., 2003. The influence of size-dependent life-history traits on the structure and dynamics of populations and communities. *Ecology Letters,* Volume 6, p. 473–487.
Degraer, S. et al., 2006. *The macrobenthos atlas of the Belgian part of the North Sea.* Brussel: Belgian Science Policy.
Donadi, S. et al., 2013. Cross-habitat interactions among bivalve species control community structure on intertidal flats. *Ecology,* Volume 94, pp. 489-498.

Duport, E., Stora, G., Tremblay, P. & Gilbert, F., 2006. Effects of population density on the sediment mixing induced by the gallery-diffusor Hediste (Nereis) diversicolor O.F. Müller, 1776. Journal of Experimental Marine Biology and Ecology. *J. Exp. Mar. Bio.,* 336(1), pp. 33-41.
Edgar, G., 1993. Measurement of the carrying capacity of benthic habitats using a metabolic-rate based index. *Oecologia,* 95(1), p. 115–121.
Ernest, S. et al., 2003. Thermodynamic and metabolic effects on the scaling of production and population energy use. *Ecol. Lett.,* Volume 6, pp. 990-999.
Fagherazzi, S. & Wiberg, P., 2009. Importance of wind conditions, fetch, and water levels on wave-generated shear stresses in shallow intertidal basins. J. *Journal of Geophysical Research,* Volume 114, p. F03022.
Fernandes, S., Sobral, P. & Costa, M., 2006. Nereis diversicolor effect on the stability of cohesive intertidal sediments. *Aquat. Ecol.,* Volume 40, p. 567–579.
Flach, E., 1996. The influence of the cockle, Cerastoderma edule, on the macrozoobenthic community of tidal flats in the Wadden Sea. *Mar. Ecol. - PSZNI,* 17(I), p. 87–98.
Friedrichs, C., 2011. Tidal Flat Morphodynamics. In: E. Wolanski & D. McLusky, eds. *Treatise on Estuarine and Coastal Science.* s.l.:Elsevier, p. 4590.
Friedrichs, M., Leipe, T., Peine, F. & Graf, G., 2009. Impact of macrozoobenthic structures on near-bed sediment fluxes. *J. Mar. Sys.,* Volume 75, p. 336–347.
Gaston, K. & Blackburn, T., 2000. *Pattern and process in macroecology.* s.l.:Blackwell Science.
Gerdol, V. & Hughes, R., 1994. Feeding behaviour and diet of Corophium volutator in an estuary in southeastern England. *Mar. Ecol. Prog. Ser.,* Volume 114, pp. 103-108.
Gillooly, J. et al., 2006. Response to Clarke and Fraser: effects of temperature on metabolic rate. *Funct. Ecol.,* 20(2), pp. 400-404.
Gillooly, J. et al., 2001. Effects of size and temperature on developmental time. *Nature,* Volume 417, pp. 70-73.
Gjoni, V. & Basset, A., 2018. A cross-community approach to energy pathways across lagoon macroinvertebrate guilds. *Est. Coast.,* 41(8), p. 2433–2446.
Gjoni, V., Cozzoli, F., Rosati, I. & Basset, A., 2017. Size–Density Relationships: a Cross-Community approach to benthic macroinvertebrates in Mediterranean and Black Sea Lagoons. *Estuaries and Coasts,* 40(4).
Glazier, D., 2005. Beyond the '3/4-power law': variation in the intra- and interspecific scaling of metabolic rate in animals.. *Biological Review,* Volume 80, p. 611–662.
Glazier, D. et al., 2011. Ecological effects on metabolic scaling: Amphipod responses to fish predators in freshwater springs. *Ecological Monographs,* 81(4), pp. 599-618.
Grömping, U., 2006. Relative importance for linear regression in R: The package relaimpo. *Journal of Statistical Softwares,* 17(1), pp. 1-27.
Grabowski, R., Droppo, I. & Wharton, G., 2011. Erodibility of cohesive sediment: The importance of sediment properties. *Earth-Science Reviews,* 105(3-4), pp. 101-120.
Guelorget, O. & Perthuisot, J., 1992. Vie et Milieu. *Paralic ecosystems. Biological organization and functioning,* Volume 42:, pp. 215-251.
Hedman, J., Gunnarsson, J., Samuelsson, G. & Gilbert, F., 2011. Particle reworking and solute transport by the sediment-living polychaetes Marenzelleria neglecta and Hediste diversicolor. *J. Exp. Mar. Biol. Ecol.,* 407(2), pp. 294-301.
Holtmann, S. et al., 1996. *Atlas of the zoobenthos of the Dutch continental shelf.* Amsterdam: Ministry of Transport, Public Works and Water Management Rijswijkwaterstaat.
Humphreys, J. et al., 2015. Introduction, dispersal and naturalization of the Manila clam Ruditapes philippinarum in British estuaries, 1980–2010. *J. Mar. Biol. Assoc. UK,* 95 (6), pp. 1163-1172.
Humphries, M. & McCann, K., 2014. Metabolic ecology. *J. Anim. Ecol.,* 83(1), pp. 7-19.

Hu, Z. et al., 2018. Dynamic equilibrium behaviour observed on two contrasting tidal flats from daily monitoring of bed-level changes. *Geomorphology.*
Hu, Z. et al., 2015. Predicting long-term and short-term tidal flat morphodynamics using a dynamic equilibrium theory. *J. Geophys. Res.-Earth Surf.,* Volume 120, pp. 1803-1823.
Ieno, E., Solan, M., Batty, P. & Pierce, G., 2006. How biodiversity affects ecosystem functioning: roles of infaunal species richness, identity and density in the marine benthos. *Mar. Ecol. Prog. Ser.,* Volume 311, pp. 263-271.
Joensuu, M. et al., 2018. Sediment properties, biota, and local habitat structure explain variation in the erodibility of coastal sediments. *Limn. Ocean.,* Volume 63, p. 173–186.
Jones, C., Lawton, J. & Shachak, M., 1994. Organisms as ecosystem engineers. *Oikos,* 69(3), p. 373–386.
Jones, C., Lawton, J. & Shachak, M., 1997. Positive and negative effects of organisms as physical ecosystem engineers. *Ecology,* 78(7), p. 1946–1957.
Kleiber, M., 1932. Body size and metabolism. *Hilgardia,* Volume 6, pp. 315-353.
Kooijman, S., 2000. *Dynamic energy and mass budgets in biological systems.* Cambridge: Cambridge University Press.
Kristensen, E., 1983. Ventilation and oxygen uptake by 3 species of Nereis (Annelida: Polychaeta). II. Effects of temperature and salinity changes. *Mar. Ecol. Prog. Ser.,* Volume 12, pp. 299-306.
Kristensen, E., 2001. Impact of polychaetes (Nereis spp. and Arenicola marina) on carbon biogeochemistry in coastal marine sediments. –. *Geochem. Trans. ,* Volume 2, p. 92–103.
Kristensen, E. et al., 2013. Influence of benthic macroinvertebrates on the erodability of estuarine cohesive sediments: Density- and biomass-specific responses. *Estuar. Coast. Shelf S.,* Volume 134, pp. 80-87.
Kupryianchyk, D. et al., 2013. Bioturbation and dissolved organic matter enhance contaminant fluxes from sediment treated with powdered and granular activated carbon. *Environ. Sci. Technol.,* 47(10), pp. 5092-10.
Le Hir, P., Monbet, Y. & Orvain, F., 2007. Sediment erodability in sediment transport modelling: Can we account for biota effects?. *Conti. Shelf Res.,* Volume 27, p. 1116–1142.
Lee, H. & Swartz., R., 1980. Biological processes affecting the distribution of pollutants in marine sediments. Part ii. Biodeposition and bioturbation. In: R. Baker, ed. *Contaminants and sediment.* s.l.:Environmental Protection Agency.
Li, B. et al., 2017. Bioturbation effect on the erodibility of cohesive versus non-cohesive sediments along a current velocity gradient: a case study on cockles. *J. Exp. Mar. Biol. Ecol.,* Volume 496, pp. 84-90.
Lindeman, R., Merenda, P. & Gold, R., 1980. *Introduction to Bivariate and Multivariate Analysis.* Glenview(IL): Scott, Foresman.
Maire, O. et al., 2006. Effects of food availability on sediment reworking in Abra ovata and A. nitida.. *Mar. Ecol. Prog. Ser.,* Volume 319, pp. 135-153.
Marquet, P. et al., 2005. Scaling and power-laws in ecological systems. *J. Exp. Biol.,* Volume 208, pp. 1749-1769.
McGill, B., Enquist, B., Weiher, E. & Westoby, M., 2006. Rebuilding community ecology from functional traits. *Trends Ecol. Evol.,* 21(4), pp. 78-185.
Meadows, P. & Reid, A., 1966. The behaviour of Corophium volutator (Crustacea: Amphipoda).. *J. Zool.,* Volume 150, pp. 387-399.
Meadows, P. & Tait, J., 1989. Modification of sediment permeability and shear strength by two burrowing invertebrates. *Mar. Biol.,* Volume 101, pp. 75-82.
Meadows, P., Tait, J. & Hussain, S., 1990. Effects of estuarine infauna on sediment stability and particle sedimentation. *Hydrobiologia ,* Volume 190, pp. 263-266.

Mehta, A. & Partheniades, E., 1982. *Resuspension of deposited cohesive sediment beds.* Cape Town, 18th Conference on Coastal Engineering ASCE.
Menezes, S., Baird, D. & Soares, A., 2010. Beyond taxonomy: a review of macroinvertebrate trait-based community descriptors as tools for freshwater biomonitoring.. *J. Appl. Ecol.,* 47(4), pp. 711-719.
Mermillod-Blondin, F. & Lemoine, D. G., 2010. Ecosystem engineering by tubificid worms stimulates macrophyte growth in poorly oxygenated wetland sediments. *Funct. Ecol.,* Volume 24, p. 444–453.
Montserrat, F. et al., 2008. Benthic community-mediated sediment dynamics. *Mar. Ecol. Prog. Ser.,* Volume 372, pp. 43-59.
Montserrat, F. et al., 2009. Sediment segregation by biodiffusing bivalves. *Est. Coast. Shelf Sci.,* 83(4), pp. 379-391.
Mouillot, D. et al., 2006. Alternatives to taxonomic-based approaches to assess changes in transitional water communities.. *Aquat. Conserv.,* Volume 16, p. 469–482.
Nascimento, I., Dickson, K. & Zimmerman, E., 1996. Heat shock protein response to thermal stress in the Asiatic clam, Corbicula fluminea. *Aquat. Ecosyst. Health,* 5(4), p. 231–238.
Nasermoaddeli, M. et al., 2018. A model study on the large-scale effect of macrofauna on the suspended sediment concentration in a shallow shelf sea. *Est. Coast. Shelf Sci.,* Volume 211, pp. 62-76.
Nilsson, H. & Rosenberg, R., 2002. Succession in marine benthic habitats and fauna in response to oxygen deficiency: analysed by sediment profile-imaging and by grab samples. *Mar. Ecol. Prog. Ser.,* Volume 197, pp. 139-149.
Ong, E., Briff, M., Moens, T. & Van Colen, C., 2017. Physiological responses to ocean acidification and warming synergistically reduce condition of the common cockle Cerastoderma edule. *Marine Environmental Research,* Volume 130, pp. 38-47.
Orvain, F., 2005. A model of sediment transport under the influence of surface bioturbation: Generalisation to the facultative suspension-feeder Scrobicularia plana. *Mar. Ecol. Prog. Ser.,* Volume 286, p. 43–56.
Orvain, F., Le Hir, P. & Sauriau, P., 2003. A model of fluff layer erosion and subsequent bed erosion in the presence of the bioturbator, Hydrobia ulvae. *J. Mar. Res.,* Volume 61, pp. 823-851.
Orvain, F., Le Hir, P., Sauriau, P. G. & S., L., 2012. Modelling the effects of macrofauna on sediment transport and bed elevation: Application over a cross-shore mudflat profile and model validation. *Est. Coast. Shelf Sci.,* Volume 108, pp. 64-75.
Pörtner, H. & Farrell, P., 2008. Physiology and Climate Change. *Science,* 332(5902), pp. 690-692.
Pearce, T., 2011. Ecosystem engineering, experiment, and evolution.. *Biol. Philos.,* Volume 26, p. 793–812.
Pearson, T. & Rosenberg, R., 1978. Macrobenthic succession in relation to organic enrichment and pollution of the marine environment. *Oceanography and Marine Biology Annual Review,* Volume 5, p. 229–311.
Peters, R., 1983. *The ecological implications of body size.* New York: Cambridge University Press.
Porter, E., Owens, M. & Cornwell, J., 2006. Effect of sediment manipulation on the biogeochemistry of experimental sediment systems. *J. Coast. Res.,* 22(6), pp. 1539-1551.
Purchon, R., 1997. *The Biology of Mollusca - 2nd Edition.* s.l.:Pergamon Press Ltd..
Queirós, A. et al., 2013. A bioturbation classification of European marine infaunal invertebrates. *Ecol. Evol.,* 3(11), pp. 3958-3985.
Queirós, A. et al., 2015. Can benthic community structure be used to predict the process of bioturbation in real ecosystems?. *Prog. Oceanogr.,* Volume 137, p. 559–569.

Quintana, C. et al., 2015. Carbon mineralization pathways and bioturbation in coastal Brazilian sediments. *Sci. Rep.,* Issue 5.
Rakotomalala, C. et al., 2015. Modelling the effect of Cerastoderma edule bioturbation on microphytobenthos resuspension towards the planktonic food web of estuarine ecosystem. *Ecol. Model.,* Volume 316, p. 155–167.
Rasmussen, E., 1973. Systematics and ecology of the Isefjord marine fauna (Denmark). *Ophelia,* Volume 11, pp. 1-507.
R-Core-Team, 2017. R: A language and environment for statistical computing.. *R Foundation for Statistical Computing, Vienna, Austria. ,* pp. https://www.R-project.org/.
Roberts, W., Le Hir, P. & Whitehouse, R., 2000. Investigation using simple mathematical models of the effect of tidal currents and waves on the profile shape of intertidal mudflats. *Cont. Shelf Res.,* 20(10-11), pp. 1079-1097.
Saint-Béat, B. et al., 2104. How does the resuspension of the biofilm alter the functioning of the benthos–pelagos coupled food web of a bare mudflat in Marennes-Oléron Bay (NE Atlantic)?. *J. Sea Res.,* Volume 92, pp. 144-157.
Savage, V. et al., 2004. Effects of body size and temperature on population growth. *American Naturalist,* Volume 163, p. 429–441.
Sgro, L., Mistri, M. & Widdows, J., 2005. Impact of the infaunal Manila clam, Ruditapes philippinarum, on sediment stability. *Hydrobiologia,* 550(1), pp. 175-182.
Solan, M. et al., 2004. Extinction and ecosystem function in the marine benthos. *Science,* Volume 306, p. 1177–1180.
Solan, M. et al., 2004. In situ quantification of bioturbation using time lapse fluorescent sediment profile imaging (f SPI), luminophore tracers and model simulation. *Mar. Ecol. Prog. Ser.,* Volume 271, pp. 1-12.
Sousa, T., Domingos, T. & Kooijman, S., 2008. From empirical patterns to theory: a formal metabolic theory of life. *Philos. T. R. Soc. of Lond. B,* Volume 363, p. 2453–2464.
Sutherland, T. & Grant, J., 1998. The effect of carbohydrate production by the diatom Nitzschia curvilineata on the erodibility of sediment. *Limnol. Ocenogr.,* 41(1), pp. 65-72.
Suykerbuyk, W. et al., 2012. Suppressing antagonistic bio-engineering feedbacks doubles restoration success. *Ecol. Appl.,* Volume 22, p. 1224–1231.
Swartz, L., 1991. Seasonal variation in body weight of the bivalves Macoma balthica, Scrobicularia plana, Mya arenaria and Cerastoderman edule in the Dutch Wadden sea. *Neth. J. Sea Res.,* 28(3), pp. 231-245.
Tagliapietra, D., Sigovini, M. & Magni, P., 2012. Saprobity: A unified view of benthic succession models for coastal lagoons. *Hydrobiologia,* 686(1), p. 15–28.
Thomsen, M. et al., 2017. Consequences of biodiversity loss diverge from expectation due to post-extinction compensatory responses. *Sci. Rep.,* Volume 7.
Thrush, S., Hewitt, J. & Herman, P., 2005. Multi-scale analysis of species-environment relationships. *Mar. Ecol. Prog. Ser.,* Volume 302, p. 13−26.
Tolhurst, T. et al., 2006. Small-scale temporal and spatial variability in the erosion threshold and properties of cohesive intertidal sediments. *Cont. Shelf Res.,* 26(3), pp. 351-362.
Ubertini, M. L. S., Gangnery, A., Grangere,́ . K. & LeGendre, R. O. F., 2012. Spatial variability of benthic-pelagic coupling in an estuary ecosystem: Consequences for microphytobenthos resuspension phenomenon. *Plos One,* Volume 7.
Valdemarsen, T., Quintana, C., Thorsen, S. & Kristensen, E., 2018. Benthic macrofauna bioturbation and early colonization in newly flooded coastal habitats. *Plos One.*

van der Meer, J. et al., 2013. Measuring the flow of energy and matter in marine benthic animal populations. In: A. Eleftheriou, ed. *Methods for the Study of Marine Benthos.* s.l.:John Wiley & Sons, pp. 326-407.
van Prooijen, B., Montserrat, F. & Herman, P., 2011. A process-based model for erosion of Macoma balthica-affected mud beds. *Cont. Shelf Res.,* Volume 31, p. 527–538.
van Prooijen, B. & Winterwerp, J., 2010. A stochastic formulation for erosion of cohesive sediments. *J. Geophys. Res.,* 115(C01005).
van Wesenbeeck, B. et al., 2007. Biomechanical warfare in ecology; negative interactions between species by habitat modification. *Oikos,* Volume 116, pp. 742-750.
Vannote, R. et al., 1980. The river continuum concept. *Can. J. Fish. Aquat. Sci.,* Volume 37, p. 130–137.
Verdelhos, T., Marques, J. & Anastácio, P., 2015. Behavioral and mortality responses of the bivalves Scrobicularia plana and Cerastoderma edule to temperature, as indicator of climate change's potential impacts. *Ecol. Ind.,* Volume 58, pp. 95-103.
Verdelhos, T., Marques, J. & Anastácio, P., 2015. The impact of estuarine salinity changes on the bivalves Scrobicularia plana and Cerastoderma edule, illustrated by behavioral and mortality responses on a laboratory assay. *Ecol. Ind.,* Volume 52, p. 96–104.
Volkenborn, N., Robertson, D. & Reise, K., 2009. Sediment destabilizing and stabilizing bio-engineers on tidal flats: Cascading effects of experimental exclusion. *Helgol. Mar. Res.,* Volume 63, p. 27–35.
Vos, P., Misdorp, R. & De Boer, P., 1998. Sediment stabilization by benthic diatoms in intertidal sandy shoals; Qualitative and quantitative observations. In: d. B. P., A. van Gelder & S. Nio, eds. *Tide-Influenced Sedimentary Environments and Facies.* s.l.:Reidel, pp. 511-526.
Walles, B. et al., 2015. The ecosystem engineer Crassostrea gigas affects tidal flat morphology beyond the boundary of their reef structures. *Estuaries Coast.,* Volume 38, pp. 941-959.
Wendelboe, K., Egelund, J., Mogens, R. & Valdemarsen, T., 2013. Impact of lugworms (Arenicola marina) on mobilization and transport of fine particles and organic matter in marine sediments. *J. Sea Res.,* Volume 76, p. 31–38.
Widdows, J. & Brinsley, M., 2002. Impact of biotic and abiotic processes on sediment dynamics and the consequences to the structure and functioning of the intertidal zone. *J. Sea Res.,* 48(2), pp. 143-156.
Widdows, J., Brinsley, M. & Pope, N., 2009. Effect of Nereis diversicolor density on the erodability of estuarine sediment. *Mar. Ecol. Prog. Ser.,* Volume 378, pp. 135-143.
Widdows, J., Brinsley, M., Salkeld, P. & Elliott, M., 1998. Use of annular flumes to determine the influence of current velocity and bivalves on material flux at the sediment-water interface. *Estuaries,* Volume 21, p. 552–559.
Willows, R., Widdows, J. & Wood, R., 1998. Influence of an infaunal bivalve on the erosion of an intertidal cohesive sediment: A flume and modeling study. *Limnol. Oceanogr.,* Volume 43, p. 1332–1343.
Winterwerp, J. & van Kesteren, W., 2004. *Introduction to the physics of cohesive sediment in the marine environment.* Amsterdam: Elsevier.
Winterwerp, J. et al., 2018. Efficient consolidation model for morphodynamic simulations in Low-SPM environments. *J. Hydraul. Eng.,* 144(8), p. 04018055.
Wrede, A. et al., 2018. Organism functional traits and ecosystem supporting services – A novel approach to predict bioirrigation. *Ecol. Ind.,* Volume 91, pp. 737-743.
Ysebaert, T. & Herman, P., 2002. Spatial and temporal variation in benthic macrofauna and relationships with environmental variables in an estuarine, intertidal soft-sediment environment. *Mar. Ecol. Prog. Ser.,* Volume 244, pp. 105-124.

Yvon-Durocher, G. et al., 2012. Reconciling the temperature dependence of respiration across timescales and ecosystem types. *Nature,* Volume 487, p. 472–473.
Zebe, E. & Schiedek, D., 1996. The lugworm Arenicola marina: A model of physiological adaptation to life in intertidal sediments. *Helgolander Meersun,* Volume 50, p. 37–68.
Zhang, L. et al., 2017. The impact of deep-tier burrow systems in sediment mixing and ecosystem engineering in early Cambrian carbonate settings. *Sci. Rep.,* Volume 7.
Zhou, Z. et al., 2015. Modeling sorting dynamics of cohesive and non-cohesive sediments on intertidal flats under the effect of tides and wind waves. *Cont. Shelf. Res.,* Volume 104, pp. 76-91.
Zhu, Z. et al., 2016. Interactive effects between physical forces and ecosystem engineers on seed burial: a case study using Spartina anglica. *Oikos,* 125(1), pp. 98-106.
Zou, K., Thébault, E., Lacroix, G. & Barot, S., 2016. Interactions between the green and brown food web determine ecosystem functioning. *Funct. Ecol.,* Volume 30, p. 1454–1465.
Zuur, A. et al., 2009. *Mixed Effects Models and Extensions in Ecology*. New York: Springer-Verlag.
Zwarts, L., Blomert, A., Spaak, P. & de Vries, B., 1994. Feeding radius, burying depth and siphon size of Macoma balthica and Scrobicularia plana. *J. Exp. Mar. Biol. Ecol.,* 183(2), pp. 193-212.
Zwarts, L. & Wanink, J., 1989. Siphon size and burying depth in deposit- and suspension-feeding benthic bivalves. *Mar. Biol.,* Volume 100, p. 227–240.

Figures

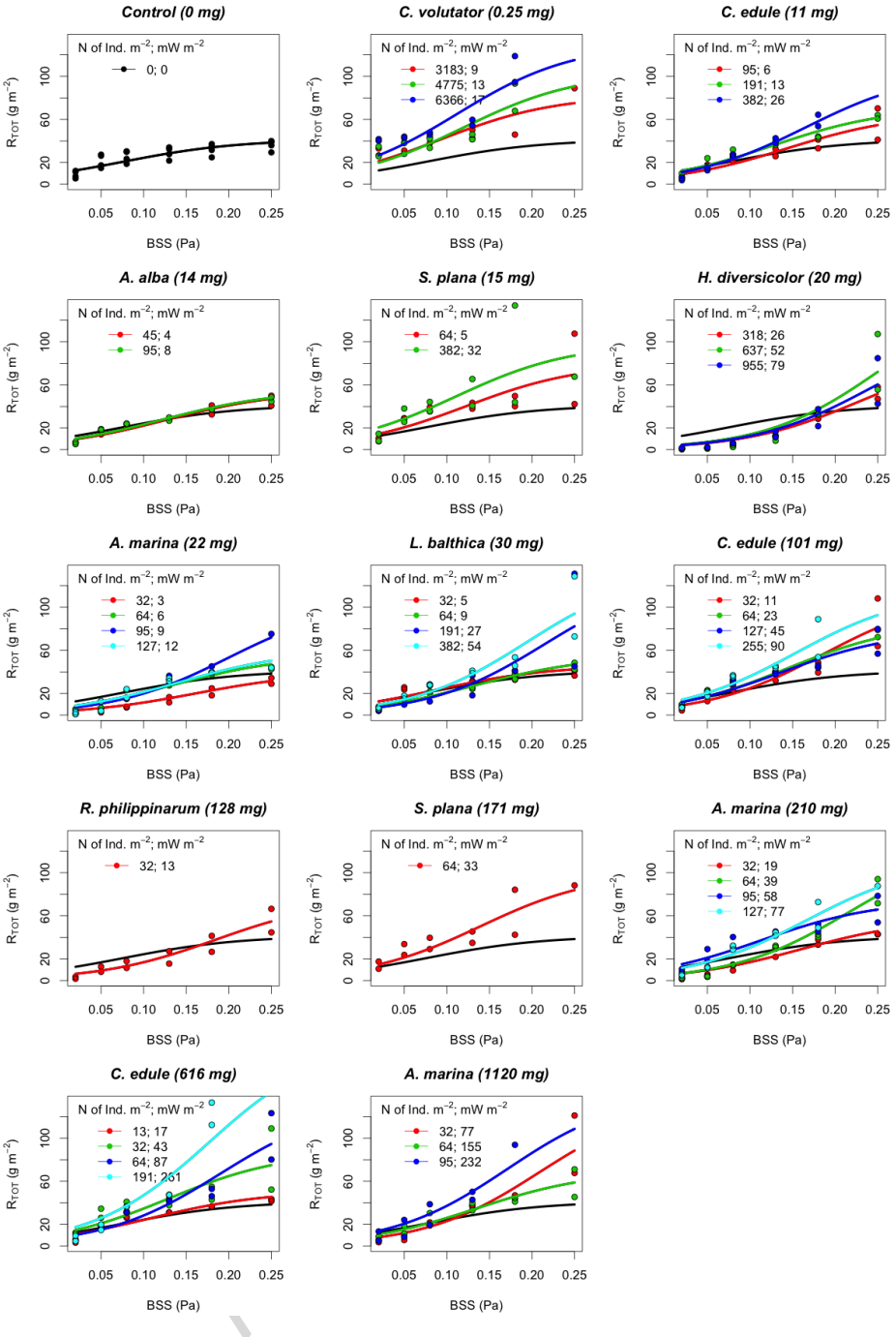

Figure 1. Relationship between R_{TOT} (total mass of suspended sediment, g m^{-2}) and Bed Shear Stress (BSS, Pa) for different species, individual sizes and densities of bioturbators (coloured lines), ordered by the individual size of the bioturbators. The black line shows the defaunated control. The relationship was modelled as a logistic sigmoidal curve $R_{TOT} \sim a/1+e^{[(b-BSS)/c]}$ allowing random variations in the asymptote *a* and midpoint *b* for each treatment (Table 2).

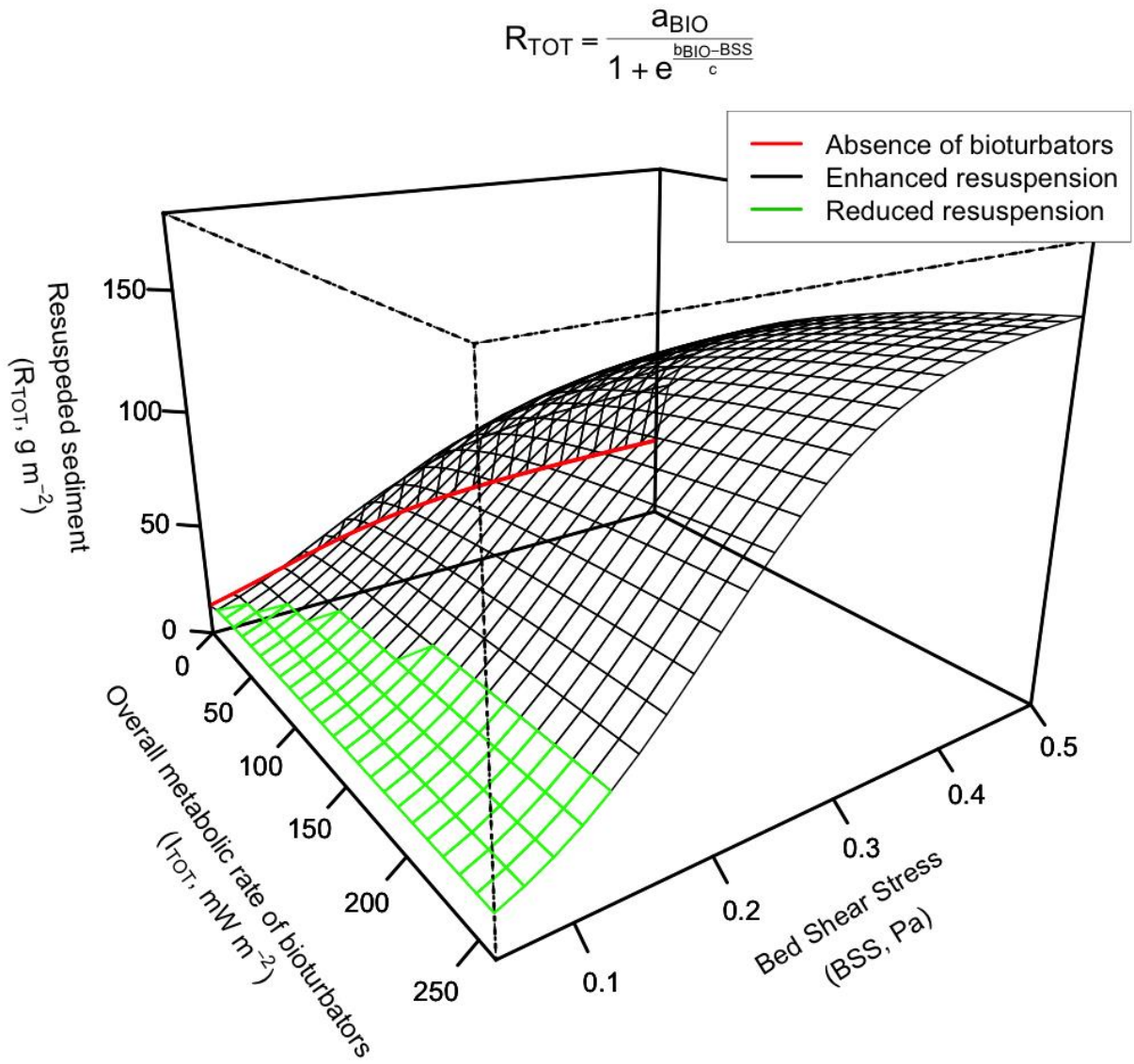

Figure 2: Relationship between amount of suspended sediment (R_{TOT}, g m^{-2}), metabolic rate of the bioturbating population (I_{TOT}, mW m^{-2}) and Bed Shear Stress (BSS, Pa). The relationship was modelled as a logistic sigmoidal curve $R_{TOT} \sim a_{BIO}/1+e^{[(b_{BIO}-BSS)/c]}$, accounting for the variation of the asymptote a_{BIO} (g m^{-2}) and the midterm b_{BIO} (Pa) at the variation of I_{TOT} as predicted from Equation 3.1 and Equation 4.1. The red line shows the defaunated control. The green part of the grid shows the conditions in which the bioturbators reduce the sediment resuspension.

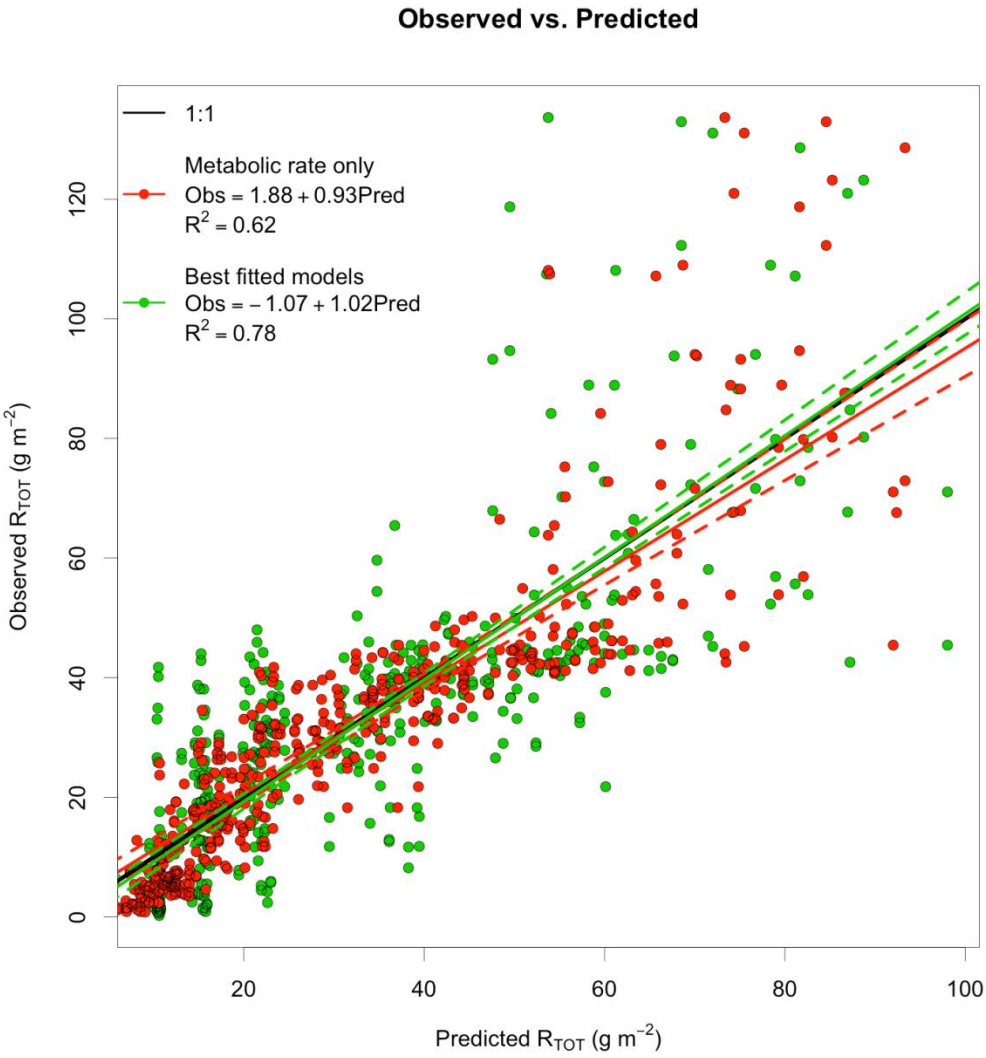

Figure 3. Relationship between observed sediment resuspension in our experiments (R_{TOT} g m^{-2}) and predictions from Equation 5: $R_{TOT} \sim a_{BIO}/1+e^{[(b_{BIO}-BSS)/c]}$. The black full line show the 1:1 ratio. Full coloured lines show the average trend; dashed lines show the 95% Confidence Interval around the average trend. The red points and lines show the prediction of Equation 5 using the metabolic rate of the bioturbations population as only descriptor for variations in a_{BIO} and $b_{BIO.}$ The green points and lines show the prediction of Equation 5 including also the negative dependence of a_{BIO} from the individual size and allowing interspecific variations in b_{BIO} (Table 5).

Tables

Table 1. Table of treatments (ordered by the individual size of the bioturbators) and estimates for the asymptote *a* (suspended sediment, R_{TOT}, g m^{-2}), the midterm *b* (Bed Shear Stress, BSS, Pa) and the constant *c* (Pa) estimated from the mixed logistic model $R_{TOT} \sim a_{BIO}/1+e^{[(b_{BIO}-BSS)/c]}$ for each treatment.

	Individual size	***Number of individuals in the flume***	***Density of individuals***	***Overall metabolic rate***	***Asymptote***	***Midterm***	***Constant***
Abbreviation	*M*	*N*	*D*	I_{TOT}	*a*	*b*	*c*
Unit	*mg AFDW*	*N of Ind.*	*N of Ind. m^{-2}*	*mW m^{-2}*	*g m^{-2}*	*Pa*	*Pa*
Species							
Defaunated control	0	0	0	0	41	0.08	0.07
Corophium volutator	0.25	500	3183	9	83	0.09	0.07
Corophium volutator	0.25	750	4775	13	104	0.12	0.07
Corophium volutator	0.25	1000	6366	17	130	0.11	0.07
Cerastoderma edule	11	15	96	6	66	0.14	0.07
Cerastoderma edule	11	30	191	13	72	0.13	0.07
Cerastoderma edule	11	60	382	26	106	0.17	0.07
Abra alba	14	7	45	4	55	0.13	0.07
Abra alba	14	15	95	8	55	0.12	0.07
Scrobicularia plana	15	10	64	5	80	0.12	0.07
Scrobicularia plana	15	60	382	32	98	0.11	0.07
Hediste diversicolor	20	50	318	26	89	0.23	0.07
Hediste diversicolor	20	100	636	52	148	0.25	0.07
Hediste diversicolor	20	150	955	79	114	0.24	0.07
Arenicola. marina	22	5	32	3	40	0.16	0.07
Arenicola. marina	22	10	64	6	56	0.13	0.07
Arenicola. marina	22	15	95	9	106	0.2	0.07
Arenicola. marina	22	20	127	12	61	0.14	0.07
Limecola balthica	30	5	32	5	46	0.09	0.07
Limecola balthica	30	10	64	9	55	0.13	0.07
Limecola. balthica	30	30	191	27	131	0.21	0.07
Limecola balthica	30	60	382	54	136	0.19	0.07
Cerastoderma edule	101	5	32	11	113	0.19	0.07
Cerastoderma edule	101	10	64	23	86	0.14	0.07
Cerastoderma edule	101	20	127	45	79	0.14	0.07
Cerastoderma edule	101	40	255	90	115	0.15	0.07
Ruditapes philippinarum	128	5	32	13	76	0.18	0.07
Scrobicularia plana	171	10	64	33	100	0.14	0.07
Arenicola. marina	210	5	323	19	58	0.16	0.07

Arenicola. marina	210	10	64	39	126	0.22	0.07
Arenicola. marina	210	15	95	58	75	0.11	0.07
Arenicola. marina	210	20	127	77	111	0.17	0.07
Cerastoderma edule	616	2	13	17	51	0.11	0.07
Cerastoderma edule	616	5	32	43	88	0.13	0.07
Cerastoderma edule	616	10	64	87	134	0.19	0.07
Cerastoderma edule	616	30	191	261	192	0.18	0.07
Arenicola. marina	1120	5	32	77	137	0.21	0.07
Arenicola. marina	1120	10	64	155	70	0.14	0.07
Arenicola. marina	1120	15	95	232	143	0.17	0.07

Table 2. Summary of the mixed logistic model R_{TOT}~*BSS*. The relationship was modelled as a logistic curve R_{TOT}~$a/1+e^{[(b-BSS)/c]}$ allowing random variations in the asymptote *a* and midpoint *b* across the full factorial combinations of bioturbators species, densities and size gradients, while the scaling coefficient *c* was kept constant.

	R_{TOT}~$a/1+e^{[(b-BSS)/c]}$			
Predictors	*Est.*		*SE*	*p*
a	92.96	4.81		<0.001
b	0.16	0.01		<0.001
c	0.07	0.00		<0.001
Random Effects				
σ^2	103.27			
$\tau_{00\ Treatment}$	1614.69			
$\tau_{11\ Treatment\ b}$	0.00			
$\rho_{01\ Treatment}$	0.54			
ICC $_{Treatment}$	0.94			
Observations	460			
Marginal R^2 / Conditional R^2	0.527 / 0.972			

Table 3: Summary of the linear ANCOVA model of the asymptote of the logistic erosion curve (a_{BIO}) fitted using the bioturbators species as categorical variable and four basic descriptors of the investigated population as continuous variables: individual size (M, mg AFDW), density of individuals (D, N of Ind. m^{-2}), total biomass (M_{TOT} mg AFDW m^{-2}) and overall population metabolic rate (I_{TOT}, mW m^{-2}). The asymptote a_{BIO} was log transformed and the continuous explanatory variables were log plus 1 transformed. The table show the estimates parameters (Est., expressed as difference from the Control value) with associated standard error (SE) and significance value (p). The left column shows the full model. The central column shows the best fitted model as selected by stepwise elimination procedure. The right column show the model fitted I_{TOT} as the only predictor.

log(a_{BIO}) ~	**Full**			**log(1+*M*)+log(1+ I_{TOT}))**			**log(1+ I_{TOT}))**		
Predictors	*Est.*	*SE*	*p*	*Est.*	*SE*	*p*	*Est.*	*SE*	*p*
Intercept (Control)	3.72	0.26	**<0.001**	3.73	0.11	**<0.001**	3.70	0.12	**<0.001**
M	-2.05	3.57	0.57	-0.09	0.03	**<0.001**			
D	-1.88	3.64	0.61						
M_{TOT}	2.21	3.32	0.51						
I_{TOT}	-0.03	0.84	0.97	0.34	0.04	**<0.001**	0.24	0.04	**<0.001**
A. alba	-1.29	3.84	0.74						
A. marina	-5.67	6.31	0.38						
C. edule	-1.21	3.95	0.76						
C. volutator	1.72	8.34	0.84						
M. balthica	-1.24	3.87	0.75						
H. diversicolor	-8.45	9.98	0.40						
S. plana	-1.12	3.91	0.78						
R. philippinarum	-1.16	3.93	0.77						
Observations	39			39			39		
R^2 / adj R^2	0.687 / 0.542			0.654 / 0.635			0.544 / 0.531		
AIC	19.183			3.030			11.841		

Table 4: Summary of the linear ANCOVA model of the midterm of the logistic erosion curve (b_{BIO}) fitted using the bioturbators species as categorical variable and four basic descriptors of the investigated population as continuous variables: individual size (M, mg AFDW), density of individuals (D, N of Ind. m^{-2}), total biomass (M_{TOT} mg AFDW m^{-2}) and overall population metabolic rate (I_{TOT}, mW m^{-2}). The continuous explanatory variables were log plus 1 transformed. The table show the estimates parameters (Est., expressed as difference from the Control value) with associated standard error (SE) and significance value (p). The left column shows the full model. The central column shows the best fitted model as selected by stepwise elimination procedure. The right column show the model fitted using I_{TOT} as the only predictor.

b_{BIO}~	**Full**			**log(1+ I_{TOT})+Species**			**log(1+ I_{TOT}))**		
Predictors	*Est.*	*SE*	*p*	*Est.*	*SE*	*p*	*Est.*	*SE*	*p*
Intercept (Control)	0.08	0.03	**0.02**	0.08	0.03	**0.02**	0.1	0.02	**<0.001**
M	-0.19	0.42	0.65						
D	-0.18	0.43	0.68						
M_{TOT}	0.22	0.39	0.58						
I_{TOT}	-0.03	0.10	0.75	0.01	0.01	0.09	0.02	0.01	**<0.001**
A. alba	-0.12	0.45	0.79	0.03	0.04	0.42			
A. marina	-0.53	0.74	0.48	0.06	0.04	0.12			
C. edule	-0.11	0.46	0.81	0.04	0.04	0.24			
C. volutator	0.11	0.98	0.91	0.01	0.04	0.82			
M. balthica	-0.11	0.45	0.82	0.06	0.04	0.14			
H. diversicolor	-0.75	1.17	0.53	0.13	0.04	**<0.001**			
S. plana	-0.14	0.46	0.77	0.02	0.04	0.57			
R. philippinarum	-0.07	0.46	0.88	0.09	0.04	0.07			
Observations	39			39			39		
R^2 / adj R^2	0.649 / 0.487			0.631 / 0.517			0.226 / 0.205		
AIC	-148.006			-152.028			-139.32		

Table 5. Linear relationship the observed values of R_{TOT} in the flume experiments and the prediction of the logistic model $R_{TOT} \sim a/1+e^{[(b-BSS)/c]}$, accounting for the effect of metabolic rate only (left column, Equations 3.1 and 4.1), including negative dependence of the asymptote a_{BIO} from the individual size (central column, Equations 3.2 and 4.1) and species specific differences in the midterm b_{BIO} (right column, Equations 3.2 and 4.2).

	Metabolic rate			**Metabolic rate + Individual size**			**Metabolic rate + Individual size + Species**		
Predictors	*Est.*	*SE*	*P*	*Est.*	*SE*	*p*	*Est.*	*SE*	*p*
Intercept	1.88	1.28	0.14	1.87	1.24	0.13	-1.07	0.98	0.28
Predicted R_{TOT}	0.93	0.03	**<0.001**	0.93	0.03	**<0.001**	1.02	0.03	**<0.001**
Observations	460			460			460		
R^2 / adjusted R^2	0.626 / 0.625			0.642 / 0.641			0.777 / 0.777		

A unified view of cohesive sediment resuspension under bioturbators influence

Authors' contribution

- Cozzoli, Francesco: Conceptualization; Data curation; Formal analysis; Investigation; Methodology; Resources; Software; Visualization; Writing - original draft
- Gjoni, Vojsava: Writing - review & editing.
- Del Pasqua, Michela: Writing - review & editing
- Zhan, Hu: Writing - review & editing.
- Ysebaert, Tom: Conceptualization; Writing - review & editing
- Herman Peter MJ: Conceptualization; Writing - review & editing; Funding acquisition; Project administration
- Bouma Tjeerd J: Conceptualization; Writing - review & editing; Funding acquisition; Project administration

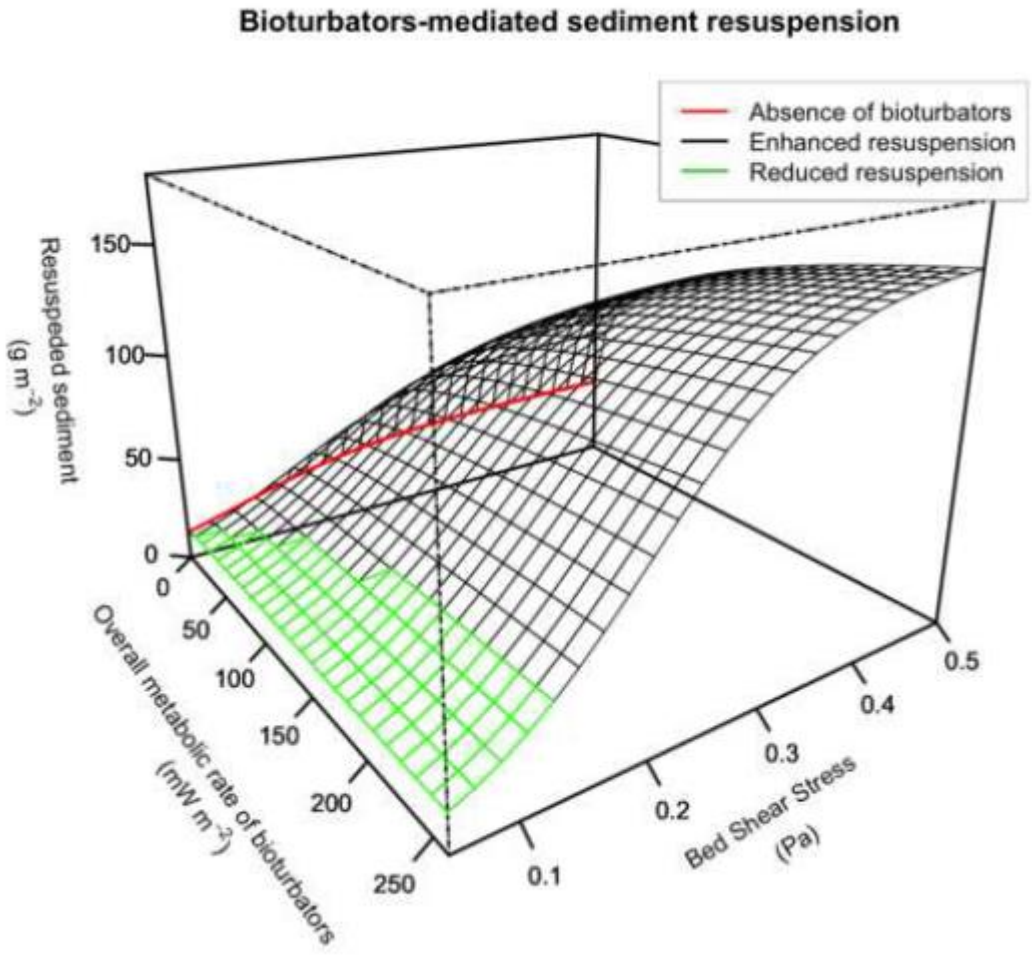

Graphical abstract

Highlights:

- Benthic infauna affect sediment erodibility *via* their bioturbating activities.
- Metabolic size scaling allows to derive general patterns of biotic effect on erosion
- The effect of different bioturbators was compared by using recirculating flumes
- The effect of bioturbators on sediment erosion can be described by their metabolism